



**HAL**  
open science

## **Science Drivers for the Future Exploration of Ceres: From Solar System Evolution to Ocean World Science**

Julie Castillo-Rogez, Marc Neveu, Vassilissa Vinogradoff, Kelly E Miller, Michael M Sori, Federico Tosi, Britney Schmidt, Jennifer E C Scully, Mohit Melwani Daswani, Kynan Hughson, et al.

### ► To cite this version:

Julie Castillo-Rogez, Marc Neveu, Vassilissa Vinogradoff, Kelly E Miller, Michael M Sori, et al.. Science Drivers for the Future Exploration of Ceres: From Solar System Evolution to Ocean World Science. The Planetary Science Journal, 2022, 3 (3), pp.64. <10.3847/PSJ/ac502b>. <hal-03858282>

**HAL Id: hal-03858282**

**<https://hal.science/hal-03858282v1>**

Submitted on 18 Nov 2022















**HAL** is a multi-disciplinary open access archive for the deposit and dissemination of scientific research documents, whether they are published or not. The documents may come from teaching and research institutions in France or abroad, or from public or private research centers.

L'archive ouverte pluridisciplinaire **HAL**, est destinée au dépôt et à la diffusion de documents scientifiques de niveau recherche, publiés ou non, émanant des établissements d'enseignement et de recherche français ou étrangers, des laboratoires publics ou privés.



HAL Authorization

# Science Drivers for the Future Exploration of Ceres: From Solar System Evolution to Ocean World Science

Julie Castillo-Rogez<sup>1</sup> , Marc Neveu<sup>2,3</sup> , Vassilissa Vinogradoff<sup>4</sup> , Kelly E. Miller<sup>5</sup> , Michael M. Sori<sup>6</sup> , Federico Tosi<sup>7</sup> ,  
Britney Schmidt<sup>8</sup> , Jennifer E. C. Scully<sup>1</sup> , Mohit Melwani Daswani<sup>1</sup> , Kynan Hughson<sup>9</sup>, Harry McSween<sup>10</sup>,  
Cristina De Sanctis<sup>7</sup> , Lynnae Quick<sup>2</sup> , Anton<sup>10</sup> Ermakov<sup>11</sup>, Guneshv<sup>10</sup> Thangjam<sup>12</sup> , Katharina Otto<sup>13</sup> , Katrin Krohn<sup>13</sup> ,  
Paul Schenk<sup>14</sup>, Andreas Nathues<sup>15</sup>, and Carol Raymond<sup>1</sup>

<sup>1</sup> Jet Propulsion Laboratory, California Institute of Technology, 4800 Oak Grove Drive, Pasadena, CA 91009, USA

<sup>2</sup> NASA Goddard Space Flight Center, 8800 Greenbelt Road, Greenbelt, MD 20771, USA

<sup>3</sup> University of Maryland, College Park, MD 20742, USA

<sup>4</sup> Aix-Marseille University, CNRS, Physics of the Interaction of Ions and Molecules Laboratory, UMR 7345, Centre Saint-jerome, 13013 Marseille, France

<sup>5</sup> Southwest Research Institute, 6220 Culebra Road, San Antonio, TX 78238, USA

<sup>6</sup> Department of Earth, Atmospheric, and Planetary Sciences, Purdue University, West Lafayette, IN 47907, USA

<sup>7</sup> Istituto Nazionale di AstroFisica, Istituto di Astrofisica e Planetologia Spaziali, Via del Fosso del Cavaliere 100, I-00133 Roma, Italy

<sup>8</sup> Department of Astronomy, Cornell University, Carpenter Hall, 313 Campus Road, Ithaca, NY 14853, USA

<sup>9</sup> University of Alaska, 3211 Providence Drive, Anchorage, AK 9950, USA

<sup>10</sup> University of Tennessee in Knoxville, Knoxville, TN 37996, USA

<sup>11</sup> Space Sciences Laboratory, University of California, Berkeley, CA 94720, USA

<sup>12</sup> School of Earth and Planetary Sciences, National Institute of Science Education of Research, Khurda, Pipli, Near, Jatni, Odisha 752050, India

<sup>13</sup> Deutsches Zentrum für Luft- und Raumfahrt, Rutherfordstraße 2, D-12489 Berlin, Germany

<sup>14</sup> Lunar Planetary Institute, Universities Space Research Association, 3600 Bay Area Boulevard, Houston, TX 77058, USA

<sup>15</sup> Max-Planck-Institut für Sonnensystemforschung, Justus-von-Liebig-Weg 3, D-37077 Göttingen, Germany

# 1                   **Science Drivers for the Exploration of Ceres:** 2                   **From Solar System Evolution to Ocean World Science**

## 3 4 5   **Abstract**

6 Dawn revealed that Ceres is a compelling target whose exploration pertains to many science  
7 themes: as a large ice- and organic-rich body, potentially representative of the population of objects  
8 that brought water and organics to the inner solar system, as well as a brine-rich body whose study  
9 can contribute to ocean world science. The Dawn observations have led to a renewed focus on  
10 planetary brine physics and chemistry based on the detection of many landforms built off or  
11 suspected to be emplaced via brine effusion. Ceres' relative proximity to Earth and direct access  
12 to its surface of evaporites evolved from a deep brine reservoir make this dwarf planet an appealing  
13 target for follow-on exploration that would address science questions pertinent to the evolution of  
14 ocean worlds and the origin of volatiles and organics in the inner solar system.

## 15       **1. Introduction**

16 In the last decade of planetary exploration, the investigation by the Dawn mission of the dwarf  
17 planet Ceres, the most water-rich body in the inner solar system after Earth and largest object in  
18 the main asteroid belt, proved to be a major milestone. Ceres has sufficient H<sub>2</sub>O and silicates (i.e.,  
19 radioisotopes) to host subsurface liquid water throughout its history, leading to a layered interior  
20 structure with a high degree of aqueous alteration (Ermakov et al. 2017; Fu et al. 2017). Deposits  
21 of bright carbonates and phyllosilicates are indicative of pervasive and global aqueous alteration  
22 (Ammannito et al., 2016; De Sanctis et al., 2016; Carrozzo et al. 2018). The Dawn mission also  
23 revealed evidence for recent and even ongoing geological activity on Ceres (Ruesch et al. 2016;  
24 De Sanctis et al. 2020), the presence of liquid – at least locally – below an ice-rich crust (Ruesch  
25 et al. 2019a; Scully et al. 2020), high concentrations of organic matter (locally) and carbon  
26 (globally) in the shallow subsurface (De Sanctis et al. 2017; Marchi et al. 2019; Prettyman et al.  
27 2017), and the presence of an exosphere and volatile transport (Villarreal et al. 2017; Formisano

28 et al. 2018). Even though the evidence for a global liquid layer in Ceres at present is circumstantial,  
29 Ceres displays evidence for the past and recent occurrence of a variety of processes that are  
30 relevant to ocean worlds.

31 This paper reviews the state of knowledge of Ceres after Dawn, including emerging interpretations  
32 about its evolution and the state of its residual liquid brine (Section 2). Then, we review how  
33 knowledge of Ceres contributes to better understanding the evolution of other large water-rich  
34 bodies and we describe the relevance of Ceres' study to other science themes (Section 3). Based  
35 on these considerations, we offer recommendations for the future research and exploration of Ceres  
36 with the purpose to further contribute to the fields of planetary origins and ocean world science  
37 (Section 4).

## 38 **2. Key Dawn Results at Ceres**

39 Pre-Dawn, Ceres was known to be a volatile-rich body that accreted ice and carbonaceous material  
40 early in the age of solar system formation (O'Brien and Sykes, 2011). Given the comparatively  
41 high temperatures on Ceres' surface, water ice sublimates when exposed at the surface and could  
42 only be detected in a few locations by Dawn, the largest located in Oxo crater (Combe et al., 2016)  
43 and the smaller patches in the northern hemisphere where persistently shadowed regions are  
44 present (Platz et al., 2016). However, the Dawn mission revealed several lines of compelling  
45 evidence for an ice-rich crust. (1) Gravity inversions yield a low crustal density of  $\sim 1200 \text{ kg/m}^3$   
46 (Ermakov et al., 2017). (2) Crater morphometry nearly exactly matches that of icy satellites  
47 (Hiesinger et al., 2016). Consideration of crater relaxation is consistent with the shallow  
48 subsurface being up to 40% ice by volume, though this ice content may vary laterally and with  
49 depth (Bland et al., 2016; Otto et al., 2019; Sizemore et al., 2019). (3) Distinct morphologic  
50 features can be attributed to a large fraction of ice in Ceres' crust. These features include known  
51 volatile-related morphologies such as fractures related to intrusion (uplift), pitted terrains and flow-  
52 like mass wasting features (Schmidt et al., 2017; Scully et al., 2017; Sizemore et al., 2019).  
53 Furthermore, the occurrence of small ring-mold craters and 100 m scale hills with pingo-like  
54 morphologies (Schmidt et al., 2020) within the Occator crater suggests localized water ice  
55 reservoirs in the shallow and lower subsurface (Krohn et al., 2018). (4) Global, pervasive aqueous  
56 alteration of surface material (Ammannito et al., 2016) and abundant morphologic evidence, such  
57 as pervasive fracturing or mounds, hint at the existence of deep liquid throughout Ceres' history.

58 Flow features have been found in and around craters. Occator’s interior exhibits extended plains  
59 of ponded material and extensive lobate materials, which may be representative of water or ice-  
60 rich flows (e.g., Krohn et al., 2016; Scully et al., 2018; Schenk et al., 2016). Those features are  
61 also found around the craters Haulani, Kupalo, Ikapati (Krohn et al., 2016), Kerwan, Yalode and  
62 Urvara (e.g., Williams, 2018; Bland, 2019). Multiple flow stages and discrete feeding sources may  
63 be consistent with a cryovolcanic origin for these flows (Krohn et al., 2016), although they are  
64 likely expressions of impact-generated melt in an icy crust (Schenk et al., 2020). (5) Detection of  
65 salt compounds, in particular sodium carbonate, locally in high concentrations (Carrozzo et al.  
66 2018), Thermodynamic models suggest that in addition to water, other volatile compounds were  
67 accreted by Ceres, in particular ammonia and carbon dioxide (De Sanctis et al., 2015; Castillo-  
68 Rogez et al., 2018).

69 While some of these individual arguments can be debated (e.g., Johnson and Sori, 2020, Zolotov  
70 2020), when taken together these convincingly show that Ceres has abundant water in ice, brines  
71 and minerals. In this section, we address salient open questions about Ceres’ interior, in particular  
72 evidence for the presence of a residual ocean or regional brine reservoirs and the nature of that  
73 environment.

## 74 **2.1 Evidence for Deep Brines in Ceres at Present and Recent Activity**

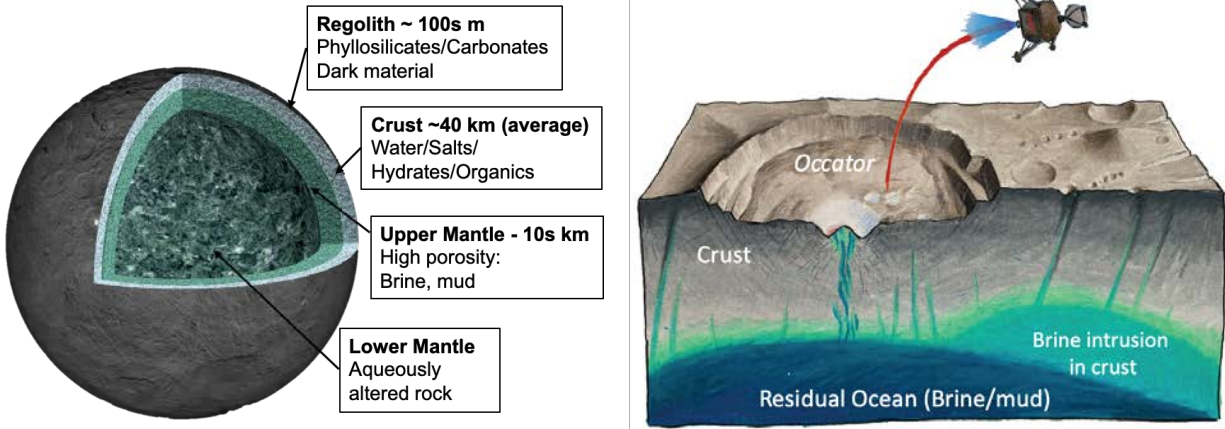
75 Both geophysical evidence and surface observations suggest the presence of brines in the  
76 subsurface. Geophysical and geological observations hint at the existence of a former subsurface  
77 ocean whose remnants are still shaping the geology of the surface today (Ruesch et al., 2019a,b

78 The Dawn geophysical data indicate that a rocky mantle starts at about 40 km below the surface,  
79 on average (between 35–55 km; Fu et al., 2017; Ermakov et al., 2017) (Figure 1). The nature of  
80 this interface, a transition to solid rock or muddy ocean, is debated. The mantle density inferred  
81 by Ermakov et al. (2017) of  $2430 \text{ kg/m}^3$  may be significantly lower than the grain density predicted  
82 by chemical modeling (Castillo-Rogez et al., 2018), suggesting possible high porosity. However,  
83 a mantle density of up to  $\sim 2800 \text{ kg/m}^3$  may be possible if Ceres has retained a fossil shape (Mao  
84 and McKinnon 2018), in which case the bulk porosity may be  $<10\text{vol.}\%$ . Additional global  
85 constraint on the presence of a deep liquid layer comes from the topography relaxation models  
86 performed by Fu et al. (2017). These authors find that a  $\sim 40\text{-}45 \text{ km}$  high-strength shell above a

87 low viscosity layer, i.e., at the top of the mantle, best reproduces Ceres' topography. However, the  
88 viscosity of the upper mantle is poorly constrained at  $<10^{21}$  Pa s.

89 Occator crater is a relatively young ( $\sim 20$  My; Neesemann et al., 2019), large crater with bright  
90 materials, including sodium carbonates and salt-rich materials, that represent evaporites from  
91 recent resurfacing ( $<2$  My; Nathues et al., 2020). The morphology of Cerealia Tholus, a  $\sim 600$  m  
92 high mound at the center of Cerealia Facula, is reminiscent of putative cryolava domes on Jupiter's  
93 moon Europa (Fagents, 2003; Quick et al., 2017). Emplacement mechanisms for the sodium  
94 carbonates and salt-rich bright materials in Occator include brine-driven cryovolcanism from a  
95 deep reservoir beneath the crust (e.g., De Sanctis et al. 2016; Krohn et al., 2016; Quick et al. 2019;  
96 Ruesch et al. 2019a) and a shallower melt chamber produced by impact-generated heat (Bowling  
97 et al., 2019; Scully et al., 2020; Schmidt et al., 2020; Raymond et al., 2020). The latter was  
98 estimated to be at least six kilometers in diameter and twenty kilometers deep (Bowling et al.,  
99 2019). The lifetime for that chamber was estimated by thermal modeling to be 10 My at most  
100 (Hesse and Castillo-Rogez, 2019) and likely much less when all evolutionary processes are  
101 accounted for. Hence, long-lived activity in Occator likely involved the contribution of a perennial  
102 deep brine reservoir whose connection with the surface was enabled by fractures created by the  
103 impact (Quick et al., 2019; Raymond et al., 2020). The dual origin for the brine can also explain  
104 the difference in evaporite deposit morphologies: at the center of the crater, Cerealia Facula is  
105 thick and continuous; whereas the Vinalia Faculae, distributed along the fractures on the eastern  
106 side of the crater floor, are thin, discontinuous, and somewhat diffuse (Ruesch et al. 2019b; Scully  
107 et al. 2020). Additionally, the existence in Occator crater of hydrated sodium chloride, a salt that  
108 dehydrates on a timescale of only centuries, suggests the presence of subsurface liquid brines today  
109 (De Sanctis et al., 2020).

110 A dozen craters, including Occator crater, display floor fractures that have been explained by  
111 shallow, cryomagmatic intrusions (Buczkowski et al., 2018, Krohn et al. 2020). Similarly to  
112 Occator, these intrusions may indicate the presence of underlying reservoirs, forming domes that  
113 uplift and fracture the overlying, brittle crater floor (Buczkowski et al., 2018, Krohn et al., 2020).



114

115 *Figure 1. Left: Current understanding of the global interior structure for Ceres after Ermakov et al. (2017) and*  
 116 *Fu et al. (2017): a strong crust overlays a briny mud and low-density rocky mantle. Right: Possible structure*  
 117 *of the crust and upper mantle inferred below the 90-km diameter Occator Crater (~50-km thick crust)*  
 118 *(Ermakov et al. 2017). The impact crater created a transient melt chamber and also introduced or reactivated*  
 119 *fractures allowing for the long-term upwelling of deep brines (Raymond et al. 2020). [Credit: J. T. Keane]*

120

121 The ~4 km tall Ahuna Mons is a steep, young mountain proposed to be a cryovolcanic construct  
 122 formed in the past tens or hundreds of Myr (Ruesch et al., 2016). Bright streaks on its flanks  
 123 contain sodium carbonates (Zambon et al., 2017). The emplacement of this large volume of  
 124 material requires a low-viscosity material (Ruesch et al., 2016). Geophysical observations indicate  
 125 that the mount material is dense and was sourced from the top of the mantle (Ruesch et al., 2019a).  
 126 These combined observations indicate an origin involving a mud- or brine-rich material. Other  
 127 mountains and domes (Buczowski et al., 2016) have also been argued to be older, degraded  
 128 cryovolcanic constructs on the basis of geophysical and geomorphological arguments (Sori et al.,  
 129 2017; 2018), although some of them may also have been formed by intrusive processes instead  
 130 (Bland et al., 2019).

## 131 2.2 Assessing Ceres' Past and Current Habitability Potential

132 In addition to the above evidence for subsurface liquid water, the surface of Ceres is blanketed  
 133 with products of the interaction between rock and liquid water, which can supply chemical energy  
 134 and bioessential elements in inorganic or organic form – the basic requirements of a habitable

135 environment. That most of the compositionally homogeneous dark surface was likely emplaced  
136 early in solar system history, whereas select areas of the surface appear geologically very recent  
137 and compositionally distinct, provides information about the habitability of environments on Ceres  
138 both in the geologic past and at recent (perhaps present) times.

139 *Bioessential elements.* Local concentration of organic carbon has been detected on the surface as  
140 a prominent 3.4- $\mu\text{m}$  spectral absorption feature and an inorganic carbon source is also available  
141 from carbonates. Combination of the data from the Dawn visible and infrared mapping  
142 spectrometer and the gamma ray and neutron detector also indicates that the global regolith  
143 contains 10 to 20 wt.% of amorphous carbon (Marchi et al., 2018). From laboratory mixtures, a  
144 similar amount is proposed (as a mixture of aliphatic and aromatic carbons) to fit the spectral  
145 abundance of the organic matter (OM) observed at Ernutet crater (De Sanctis et al., 2019). The  
146 large amount of such organic matter and amorphous carbon found in the regolith may be  
147 representative of the crust composition or may have been concentrated by an unknown mechanism.  
148 Nitrogen has been detected as a constituent of ammonium salts. The possible presence of sulfate  
149 salts provides a potential source of S. If the core is chondritic, then S and P can be inferred (for  
150 example as sulfides and schreibersite, respectively). O and H are implied as components of  
151 organics, sulfates, ammonium salts. Aliphatic-dominated organic matter has been found in the  
152 region of Ernutet crater with at least 3–4 times greater abundance than in carbonaceous chondrites  
153 (Kaplan et al., 2018; De Sanctis et al., 2019). The precise composition of this OM could not be  
154 derived from the Dawn observations. However, the mixing of the organic signatures found at  
155 Ernutet crater with other surface material (phyllosilicates, carbonates) suggests these organics  
156 formed inside Ceres (De Sanctis et al. 2019) although an exogenic origin cannot be definitely  
157 discarded.

158 *Chemical energy.* Theoretical energy sources could be provided by organics on their own  
159 (fermentation) or as half-reactions with sulfates, for example, in anaerobic respiration. However,  
160 these assessments require greater knowledge of the chemistry of the organic material. Other  
161 sources of chemical energy are possible (see Section 3.1).

162 *Habitability potential early in solar system history.* The overall homogeneity of Ceres' heavily  
163 cratered surface suggests a global emplacement at an early time when liquid water was ubiquitous  
164 in Ceres' interior, with short-lived radionuclides and accretional energy as possible heat sources

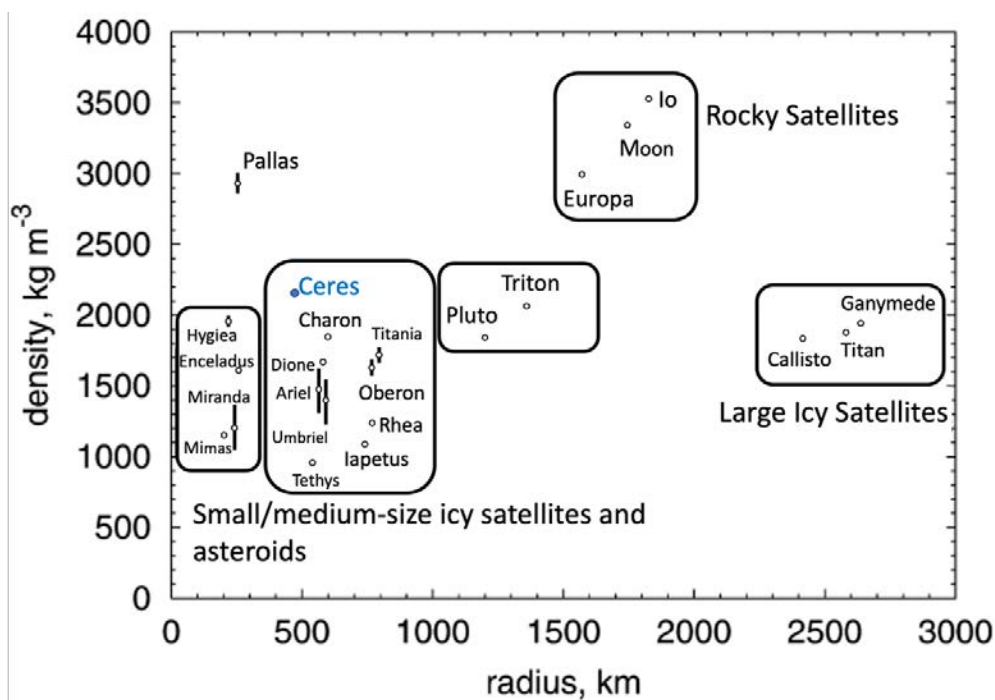
165 (e.g., Castillo-Rogez et al., 2010; Neveu and Desch, 2015; Travis et al., 2018; Castillo-Rogez et  
166 al., 2019). That dark surface is mainly composed of an unknown darkening agent (likely carbon  
167 and/or Fe compounds; Marchi et al., 2019), Mg-bearing serpentine, ammonium-bearing clays, and  
168 Ca- and/or Mg-bearing carbonates (De Sanctis et al., 2015; Ammannito et al., 2016). Modeling  
169 suggests that these compounds can together result from the complete reaction between liquid water  
170 and chondritic material in presence of CO<sub>2</sub> and NH<sub>3</sub>, which generates alkaline conditions (pH >  
171 7). Specifically, and although this remains to be confirmed experimentally, the presence of NH<sub>4</sub>  
172 suggests formation at pH > 10 and temperatures lower than 50°C, yielding ionic strengths of order  
173 0.1-1 (Neveu et al., 2017; Castillo-Rogez et al., 2018). It may be that earlier conditions were hotter  
174 but that the incorporation of ammonium into clays occurred at later, colder conditions. Early redox  
175 conditions are constrained to hydrogen fugacities between 10<sup>-8</sup> and 10<sup>-5</sup> bar by the coexistence of  
176 relatively oxidized carbonates and of relatively reduced nitrogen (as ammonium clays), as well as  
177 amorphous or organic carbon (Neveu et al., 2017; Castillo-Rogez et al., 2018).

178 *Habitability potential today.* The current physicochemical conditions of Ceres' brine reservoirs or  
179 residual liquid layer, if it exists, are not well constrained. Bounds can be derived on temperature  
180 based on the mineralogy observed in recently exposed evaporites. Minerals displayed by the  
181 Occator faculae display sodium carbonate (>70 vol.%), ammonium chlorides (up to 7 vol.%), and  
182 in the case of Cerealia Facula, a few percent of hydrohalite (Raponi et al., 2019; De Sanctis et al.,  
183 2020). At Ahuna Mons, sodium carbonate has been found at a level of 7–10vol.% (Zambon et al.,  
184 2017). These observations suggest that the source temperature should be at least 245 K (Castillo-  
185 Rogez et al., 2019). On modern Ceres, although sodium carbonate is indicative of an alkaline  
186 environment (pH~7-10; Castillo-Rogez et al., 2018) and surface expression of cryovolcanism  
187 points to subsurface liquid reservoirs on the verge of complete freezing, more specific constraints  
188 are lacking on the conditions (redox, pH, ionic strength, temperature, etc.) in Ceres' deep, cold,  
189 concentrated brines and whether that environment is within the limits that psychrophilic and  
190 halophilic organisms can tolerate (e.g., Pikuta et al., 2007).

### 191 **3. Big Picture significance – Contribution of Ceres Science to Other Fields**

192 As an ice-rich body, a dwarf planet, and the largest member of the main asteroid belt, the  
193 exploration of Ceres provides insights into properties and processes that affect all three populations  
194 of planetary bodies (Figure 2). In that respect, Ceres is unique in the solar system. Ceres shows

195 many similarities to ocean worlds in the outer solar system per its differentiated interior and brine  
 196 composition that is partly similar to Enceladus' plume grains (Postberg et al., 2011; De Sanctis et  
 197 al., 2016). Recent and likely ongoing exposure of evaporites in Occator Crater makes it a  
 198 compelling place for testing habitability paradigms by determining the environmental properties  
 199 of Ceres' residual ocean, either with in situ exploration and/or with sample return. Furthermore,  
 200 Ceres is a likely representative of the population of planetesimals that brought organics and water  
 201 to the inner solar system and might even be an example of large planetesimals that supplied Earth  
 202 with the majority of its volatiles (e.g., De Sanctis et al., 2015; Budde et al., 2019). Lastly, in  
 203 situ/sample return exploration of Ceres in the next decade would be complementary to the ongoing  
 204 sample return missions from C-type near earth asteroids (NASA's OSIRIS-REx, JAXA's  
 205 Hayabusa-2) and to ocean world missions in the outer solar system that will be launched in the  
 206 mid-2020s (NASA's Europa Clipper and Dragonfly, ESA's Jupiter Icy Moons Explorer).



207  
 208 *Figure 2. Basic physical properties for ice-rich bodies (and Io) highlight similarities between Ceres and mid-*  
 209 *sized icy moons (Figure based on Hussmann et al., 2006). Hence, knowledge gained at Ceres can inform*  
 210 *the evolution of icy moons, and vice versa.*

212

### 213 **3.1 Contribution of Ceres Exploration to Ocean World Science**

#### 214 **Extent of Internal Evolution in Water-Rich Bodies**

215 Insights to date from laboratory investigations of planetary materials indicate lesser degrees of  
216 aqueous alteration than inferred for Ceres. Thus, Ceres provides an opportunity to understand the  
217 effects of water-rock interaction at higher proportions of water relative to rock on the internal  
218 evolution of worlds with a water content similar to, or approaching, that of ocean worlds in the  
219 outer solar system (Figure 2).

220 Among planetary materials investigated in the laboratory, the CM and CI carbonaceous chondrites  
221 were likely formed in relatively small (<100 km diameter) planetesimals (Brearley, 2006).  
222 Alteration scales for these chondrites are based mainly on petrologic compositions (Browning et  
223 al., 1996; Rubin et al., 2007) and modal proportions (Howard et al., 2015), and to some extent on  
224 the abundances and isotopic compositions of volatiles (Alexander et al., 2013). A progressive  
225 sequence of reactions first produces Fe-serpentine and tochilinite, which are then converted to Mg-  
226 serpentine, magnetite, clay, and sulfates (Howard et al., 2011). Organic matter is modified and  
227 carbonates are also produced during alteration (see for example Alexander et al., 2015). In CM  
228 and CI parent bodies, these reactions occurred at relatively low temperatures and, although they  
229 required liquid water, the water:rock ratios were low and water did not separate from rock on a  
230 global scale.

231 The alteration mineralogy determined from Ceres' surface spectra is similar to the most highly  
232 altered carbonaceous chondrites but is more extreme (McSween et al., 2018). Ceres is spectrally  
233 similar to a few other C-class asteroids which may have also experienced extensive aqueous  
234 alteration, such as 10 Hygiea (e.g., Rivkin et al., 2014). These bodies, like Ceres, are among the  
235 largest asteroids, suggesting that the degree of alteration (and differentiation) of water-bearing  
236 planetesimals is related to size (McSween et al., 2018). Although the alteration mineralogy of even  
237 larger ocean worlds is not well constrained, Ceres serves as a bridge linking smaller, altered but  
238 undifferentiated planetesimals to larger bodies with subsurface oceans.

239 Neveu and Desch (2015) assumed aqueous alteration of a CM chondrite precursor by NH<sub>3</sub>-bearing  
240 fluid. In their model, hydrated chondrules sank to form a rocky core, leaving an overlying muddy  
241 mantle consisting of ice and aqueously altered fines. Castillo-Rogez et al. (2018) used  
242 thermodynamic models of a carbonaceous chondrite precursor to determine that Ceres' surface  
243 mineralogy reflects advanced alteration under high hydrogen fugacity and the mineralogy shows  
244 a weak dependence on pressure. They also predicted clathrate hydrates in the interior, which could  
245 explain the low density and high strength of the crust inferred from geophysical observations.  
246 Although the global uniformity of the surface mineral compositions (Ammannito et al., 2016)  
247 implies that the surface assemblage was excavated from depth, evidence for iron fractionation in  
248 the crust (Prettyman et al., 2017) suggest the surface mineralogy may not be representative of the  
249 mantle (Castillo-Rogez et al., 2018).

250 A key question is the extent of thermal evolution of the mantle and whether it reached metamorphic  
251 conditions leading to partial dehydration. Ceres' mantle density is uncertain, between 2400-2800  
252 kg/m<sup>3</sup> (Ermakov et al. 2017; Mao and McKinnon 2018). A dehydrated mantle composed of olivine  
253 and pyroxene would produce a bulk density higher than observed for Ceres, so, it is possible the  
254 mantle did not dehydrate, some fluid must have been retained to allow retrograde formation of  
255 some hydrous phases, or the mantle has retained some porosity filled in by brines. The presence  
256 of amphibole (tremolite), chlorite (clinochlore), and serpentine (chrysotile) in a carbonaceous  
257 chondrite clast in a ureilite breccia implies greenschist-facies metamorphism at a temperature and  
258 pressure higher than for other CM and CI chondrites, possibly consistent with conditions in the  
259 interior of a Ceres-sized asteroid (Hamilton et al., 2020). That parent body is considerably larger  
260 than envisioned for other carbonaceous chondrites, so the meteorite likely provides insights into  
261 Ceres' deep interior. Multiple reports for the presence of dehydrated material on the surface of  
262 Ceres (e.g., De Sanctis et al. 2015; Raponi et al. 2021) might be evidence for thermal  
263 metamorphism in the mantle. However, the emplacement of that material into Ceres' regolith  
264 remains to be explained. Contamination from exogenic material that may include anhydrous or  
265 dehydrated material is another possible explanation (Marchi et al. 2018).

### 266 **Long-term persistence of liquid water in the absence of tidal heating**

267 Tidal dissipation is thought to enable subsurface liquid water and related surface activity on many  
268 solar system moons, such as Enceladus and perhaps Mimas and Dione in the Saturn system,

269 possibly Miranda and Ariel in the Uranian system, and on Neptune's moon Triton (e.g., Hendrix  
270 et al., 2019). On larger objects such as Europa, Ganymede, Callisto, and Titan, radiogenic heating  
271 alone can maintain the subsurface oceans whose signatures were detected by the *Galileo* and  
272 *Cassini* missions, although tidal dissipation may enhance associated activity, e.g., at Europa.  
273 Ceres, which does not orbit a giant planet, never experienced any significant heating from tidal  
274 dissipation. That its interior still harbors liquid water on the verge of refreezing is therefore very  
275 informative of the ability of radiogenic heating, augmented perhaps to a small extent by the heat  
276 of accretion (Bierson et al., 2020) and later impacts (Bowling et al., 2019), to sustain subsurface  
277 liquid water.

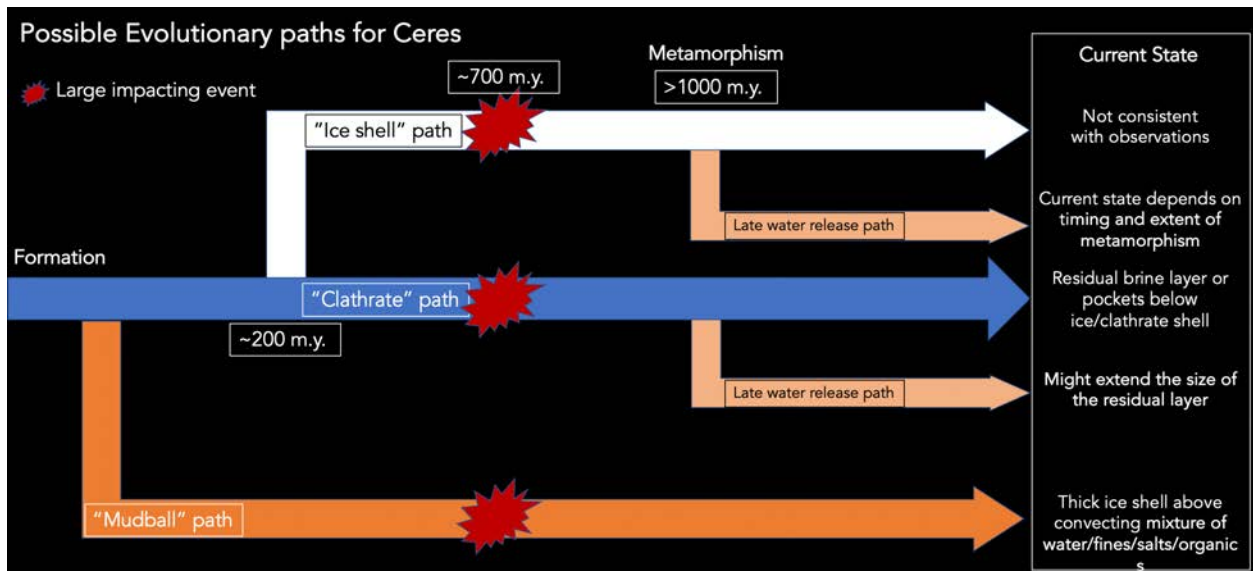
278 In the absence of tidal heating, the persistence of liquid water mainly depends on the body's size  
279 (the ratio of heat production – which scales with volume – to heat loss – which scales to first order  
280 with surface area – being proportional to the radius); the rock mass fraction, which determines the  
281 abundance of long-lived radioisotopes; the presence of salt, hydrates, or volatile impurities able  
282 to change the interior's physical and chemical properties (freezing point, insulation, strength); and  
283 to a lesser extent the heliocentric distance that largely sets the temperature at the surface  
284 (Hussmann et al., 2006). The evidence at Ceres (radius of 470 km) therefore suggests that larger  
285 worlds (radius > 700 km) such as Uranus' moons Titania and Oberon, and transneptunian objects  
286 such as Pluto, Eris, Haumea, and Makemake may, too, host subsurface liquid today. Indeed, there  
287 are hints that Pluto may harbor an ocean (Nimmo et al., 2016; Keane et al., 2016; Denton et al.,  
288 2021). On the other hand, Pluto's moon Charon, with a radius  $\approx$  600 km and heliocentric distance  
289 of  $\approx$ 40 AU, seems to have fully refrozen (Desch and Neveu, 2017).

290 An object's size and heliocentric distance are readily determined, but the crux of estimating ocean  
291 persistence in the absence of obvious surface expression or major tidal dissipation lies in  
292 understanding the feedbacks between interior physical and chemical processes. The recent  
293 exploration of Ceres (and of the Pluto system) has hinted at how complex such feedbacks may be.  
294 Salts and gas hydrates possibly affect the near-surface strength (Bland et al., 2016) and therefore  
295 the means by which heat is transferred to the surface and lost to space by convection (Formisano  
296 et al., 2020) or conduction (Neumann et al., 2020; Kamata et al., 2019). Water-rock reactions,  
297 including those able to produce Ceres' surface composition, may change the distribution of  
298 radionuclides and generate or consume antifreeze species (Neveu et al., 2017), as well as enhance

299 or inhibit deep convection in porous rock, which tends to homogenize temperatures in the interior,  
300 keeping ice melted at depth (Neveu et al., 2015). The relative densities of the crust and subsurface  
301 fluids, which depend on their chemical composition, affects the surface expression of fluids  
302 through volcanism (Ruesch et al., 2019a). Ceres offers the opportunity to investigate how this  
303 interplay of planetary physics and chemistry affects the persistence of oceans and their surface  
304 expression, with the tidal heating variable separated out.

305 The energy source driving late activity in Ceres is not well understood. Long-lived radioisotopes  
306 by themselves would not be able to preserve a deep liquid layer, especially if the shell is convecting  
307 heat. In most models, the bulk of the ocean would freeze on a timescale of about 200 million years.  
308 However, a residual liquid layer enriched in ammonia and chlorides could exist as a minimum,  
309 based on pre-Dawn models (Castillo-Rogez and McCord, 2010; Neveu and Desch, 2015). Three  
310 explanations have been suggested for the existence of substantial liquid, at least locally, inside  
311 Ceres at present (Figure 3).

312 First, the possibility that convection onset in Ceres' crust was precluded based on the inference  
313 that the crust is at least three orders of magnitude stronger than water ice (Bland et al., 2016), even  
314 though its density is only slightly greater than that of water ice. Two interpretations have been  
315 suggested: the shell is enriched in clathrate hydrates, whose thermophysical properties are  
316 consistent with these observations (Bland et al., 2016; Fu et al., 2017) and that are expected to  
317 form in Ceres' early ocean (Castillo-Rogez et al., 2018); as an alternative, pinning of the ice grain  
318 boundaries with silicate particles could also increase the overall strength of the crust (Qi et al.,  
319 2018). The main difference between the two models is that the thermal conductivity of clathrate  
320 hydrates is also a factor 5 to 10 lower than ice. Hence the clathrate-rich model would lead to  
321 warmer interiors than the ice-rich crust model (Castillo-Rogez et al., 2019).



322

323 *Figure 3. Possible explanations that have been suggested for explaining late activity in Ceres. All three*  
 324 *scenarios assume a similar early evolution involving global melting from short-lived radioisotope decay heat.*  
 325 *The top pathway is based on pre-Dawn models that assume an ice-dominated shell that might be convecting.*  
 326 *In those models, thermal metamorphism was expected to happen but not fully modeled. The middle pathway*  
 327 *assumes a shell rich in clathrate hydrates or ice-rock mixture such that convection onset is unlikely. That*  
 328 *path enables the preservation of brines, with the potential addition of volatiles produced from thermal*  
 329 *metamorphism. The bottom pathway assumes Ceres' heat transfer was driven by slow hydrothermal*  
 330 *circulation in a thick ocean that remains at present. In that case, the mantle temperatures remain too low*  
 331 *(<100°C) for thermal metamorphism to develop.*

332 The second hypothesis for explaining the presence of liquid in Ceres at present is the release of  
 333 volatiles as a consequence of thermal metamorphism in the mantle (Melwani Daswani et al., 2021).  
 334 This prospect was considered in several pre-Dawn models but its consequences on the state of the  
 335 hydrosphere was not fully modeled. The timing of that event depends on the properties of the rocky  
 336 mantle, and in particular its thermal conductivity, a parameter that is not well constrained. Hence,  
 337 a wide range of evolution outcomes are possible. The most likely period for the onset of thermal  
 338 metamorphism would be around 1 Gy, the time at which accumulated radiogenic heat reaches a  
 339 maximum before decreasing as heat transport outpaces the exponentially decreasing heat  
 340 production (Castillo-Rogez and McCord, 2010). Whether liquid release at the base of the crust or  
 341 added to the residual ocean at the time would be preserved until present remains to be modeled.

342 Third, a different evolution pathway was proposed by Travis et al. (2018) whose “mudball” model  
343 assumes long-lived convection of an ocean loaded in silicate particles. In that model, a thick ocean  
344 remains until present and the mantle temperature remains below 100°C throughout Ceres’ history.  
345 Pros and cons for that model are summarized in Castillo-Rogez and Bland (2021). The main open  
346 question is whether fine rock particles would remain in suspension for billions of years and avoid  
347 processes such as hydrolysis (Sirono, 2013) and flocculation (e.g., Kranck, 1973).

348 On top of these global evolution models, impacts may also act in creating transient melt (e.g.,  
349 Bowling et al., 2019). In particular, basin-forming impacts in Ceres’ early history (Marchi et al.,  
350 2016) likely created a significant amount of deep melt although this process and its consequences  
351 have not been modeled.

352 All of these processes are relevant to icy bodies and have already been proposed for some of them.  
353 For example, clathrate hydrates have been suggested as potentially being responsible for the  
354 preservation of liquid of other bodies with limited heat budget, such as Pluto and Callisto (Kamata  
355 et al., 2019). The occurrence of clathrate hydrates in icy moons has been predicted by previous  
356 models, e.g., Titan (Lunine and Stevenson, 1985, 1987) and Enceladus (Fortes, 2007) but their  
357 detection remains elusive. A future mission to Ceres that brings the geophysical tools necessary to  
358 probe Ceres’ subsurface could distinguish between a clathrate-rich and an ice-rich crust.

### 359 **Chemical evolution of water-rich worlds**

360 Ceres’ small heliocentric distance relative to other water-rich objects (e.g., icy moons of the giant  
361 planets and transneptunian objects) is such that water ice is not stable at its surface. Hence, the  
362 large deposit on Ceres’ surface exposes products of water-rock interaction (including salts,  
363 phyllosilicates, carbonates, oxides, volatile and organic compounds) that are telling about chemical  
364 evolution (Section 2.1). By contrast, at other water-rich worlds, hints of non-ice compounds are  
365 instead largely diluted or masked by surface water ice, especially in the case of salts. This  
366 complicates even a first-order assessment of their chemistry unless non-ice materials are expressed  
367 in another way (e.g., the plume of Enceladus, or – for volatiles – the atmospheres of Titan, Triton,  
368 and Pluto), and some non-ice components may be radiation products rather than reflective of  
369 planetary interior chemistry (e.g., Brown and Hand, 2013).

370 It follows that the chemical investigation of Ceres, which has bulk properties (density  $\approx 2000$  kg/  
371  $\text{m}^3$ ; volume-averaged radius 470 km) broadly similar to many water-rich moons and dwarf planets  
372 (densities  $\approx 1000\text{--}3000$  kg/ $\text{m}^3$ ; radii  $\approx 200\text{--}2500$  km, e.g., Hussmann et al., 2006; Figure 2),  
373 provides a unique window into their water-rock chemistry. This includes an inference of the  
374 starting rocky and icy materials that these worlds accreted, the products of their interaction, and  
375 the partitioning of these products between the interior (solids and aqueous solution), surface, and  
376 outgassing.

377 In making such extrapolations, it is important to consider possible sources of differences in  
378 chemical evolution. A first source is the diversity of formation conditions as suggested by, e.g.,  
379 the factor-of-three diversity in bulk densities across water-rich worlds. A second is a diversity of  
380 evolution pathways linked to different dynamical environments (collisions, tidal interactions) or  
381 heliocentric distances (e.g., affecting volatile escape). Nonetheless, the broad similarity between  
382 the observed or inferred distribution of these products at Ceres relative to other water-rich bodies  
383 confirms the usefulness of Ceres in providing information about the chemistry of other water-rich  
384 worlds (Neveu et al., 2017). The variety of surface ages on Ceres (Section 2.1) facilitates an  
385 assessment of the chemical changes that occurred throughout the significant fraction of solar  
386 system history spanned by these ages.

387 Several processes that affect the long-term evolution of Ceres' ocean (Figure 3) are also relevant  
388 to other mid-sized and large icy moons. First, a freezing ocean concentrates solutes, leading to  
389 saturated solutions, as might be the case for Ceres. Chemical alteration could proceed to  
390 equilibrium in Ceres, after which the ocean system would become chemically nonreactive. Release  
391 of mantle volatiles to the ocean by thermal metamorphism (Melwani Daswani et al., 2021), as well  
392 as radiolysis (e.g., Bouquet et al., 2017; Altair et al., 2018), can reintroduce chemical gradients  
393 into the ocean and/or shift ocean redox and pH conditions, maintaining limited disequilibrium  
394 (Figure 4). The effect of mantle devolatilization may be small in the case of a thick ocean but could  
395 be significant in the case of a residual liquid layer, as is expected in Ceres if the brine temperature  
396 is significantly below 273 K (Castillo-Rogez et al., 2019). Lastly, large impacts could potentially  
397 reach Ceres' ocean, at least when the crust was thinner, and introduce diverse material serving as  
398 substrate for late aqueous alteration.

399 The composition of evaporites recently exposed on Ceres' surface would inform the deep brine  
 400 reservoir environmental conditions (Castillo-Rogez et al., submitted) and test whether these  
 401 indicate a primary origin (residual endogenic liquid) or result instead from a second generation of  
 402 liquid (e.g., impact melt). In order to fully investigate the nature of the brines, spatial variations of  
 403 their texture, mineralogical, isotopic, elemental measurements, and phase relationships need to be  
 404 resolved at the nanoscale (see Chan et al., 2018).

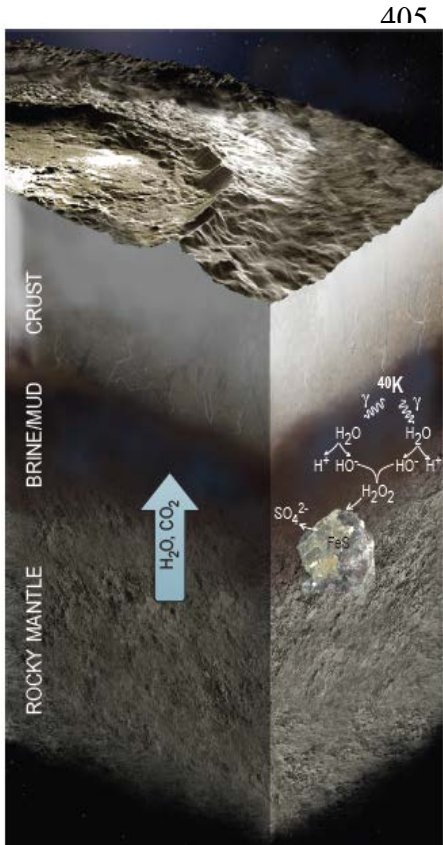


Figure 4. Summary of processes that may alter the chemical properties of a deep ocean over time: loss of volatile from the mantle upon thermal metamorphism, radiolysis, and impacts. Based after Altair et al. (2018); background rendering from Raoul Ranoa).

417

418 **Carbon partitioning and fate of organic matter in long-lived liquid reservoirs**

419 Organic matter (OM) in carbonaceous chondrites and carbonaceous interplanetary dust particles  
 420 presents a high diversity of several thousands of organic compounds with structural and molecular  
 421 continuum (Remusat et al., 2015; Alexander et al., 2017). In carbonaceous chondrites, which have  
 422 been more extensively studied, organic matter is usually divided into two fractions: i) a soluble  
 423 organic fraction (SOM), made of thousands of different small molecules (including carboxylic  
 424 acids, amino acids, sugars, aliphatic, alcohols, e.g., Schmitt-Kopplin et al., 2010); ii) an insoluble

425 organic fraction (IOM), represented as a macromolecular structure composed of aliphatic and  
426 aromatic carbon units with some heteroatoms (O, N, S) showing a high degree of cross-linking  
427 (Remusat et al., 2010) in interaction with a more volatile aromatic fraction containing molecular  
428 diversity (Danger et al., 2020). The diversity and abundance of organic matter identified to date in  
429 carbonaceous chondrites may both reflect a diversity of organic materials present in the protosolar  
430 nebula before planetary accretion (e.g., Kerridge 1999), and further enhancement via hydrothermal  
431 synthesis in chondritic parent bodies at conditions revealed in their mineral makeup (e.g., Brearley,  
432 2006). The degree of organic matter transformation during hydrothermal activity is a major  
433 question in astrochemistry with implications for carbonaceous asteroids, Ceres, icy moons, as well  
434 as Mars' surface. The analysis of CM chondrites indicate that the proportion of IOM in CM  
435 chondrites diminishes with increasing alteration, while carbonate abundance increases  
436 concomitantly (Alexander et al. 2015), indicating a degradation of OM. Also, for amino acids  
437 found in some specific CC meteorites, such as CI, CM, CR, and the ungrouped Tagish Lake (e.g.,  
438 Pizzarello et al., 2001, Pizzarello and Holmes, 2009), the relative abundance of amino acids  
439 declines with increasing degree of alteration in the CC, indicating that aqueous alteration processes  
440 altered the organic matter (Glavin et al. 2010).

441 Experimental studies showed that organic molecules are transformed during simulated aqueous  
442 activity (Kebukawa et al., 2013, 2020; Vinogradoff et al., 2018), producing numerous new soluble  
443 molecules and an insoluble organic matter with time and temperature. The nature and extent of  
444 organic matter evolution likely depends on the nature of the molecules, the interaction with the  
445 minerals, and the fluid properties (Vinogradoff et al., 2020; Haas et al., 2020; Gil-lozano, 2020).  
446 The correlation of organic material with phyllosilicates and carbonates observed at the surface of  
447 Ceres (De Sanctis et al., 2019; Raponi et al., 2017), suggests a close relationship between these  
448 phases and a possible co-evolution during hydrothermal processing. Ceres being the first main belt  
449 object at which strong and incontestable OM signature has been detected, further observations and  
450 analysis of this assemblage is of primary importance for understanding the evolution of organic  
451 matter in hydrothermal systems. Quantifying the extent of organic matter transformation in Ceres  
452 requires new observations, models and experiments in order to better constrain the role of the  
453 abundance of minerals, the water to rock ratio, and the salinity. Developing that knowledge will  
454 also be valuable for predicting the chemical evolution of organic material in carbonaceous-rich  
455 asteroids and ocean worlds.

456 Observations of organic matter in carbonaceous chondrites reveal a close association of likely  
457 soluble compounds with minerals, especially Mg-phyllsilicates after hydrothermal alteration (Le  
458 Guillou et al., 2014; Vinogradoff et al., 2017). Considering the similar composition of organic  
459 matter on Ceres' surface and its association with silicates, the differentiation event may have led  
460 to accumulation of organic matter in the rocky crust, simultaneously to geochemical processes.  
461 Fundamental thermodynamic considerations identify graphite, methane, and carbonate as the  
462 stable endmember carbon compounds depending on geochemical parameters including  
463 temperature, redox state, and pH, and assuming a long-lived system. Kinetic factors may play a  
464 role in the long-term evolution of natural carbon systems, and metastable organic compounds, such  
465 as kerogen of intermediate oxidation state (Seewald et al., 1998), may be important carbon  
466 reservoirs on long timescales (e.g., Shock & McKinnon, 1993; Neveu et al., 2017). Increased  
467 temperature, clay catalysts, and increased brine concentration tend to make water a better solvent  
468 for organics, and as a result the organics tend to be more reactive (less stable) in those  
469 environments (Siskin and Katritzky, 2001). On the other hand, if the system stayed cold, for  
470 example, then even over billions of years the kerogen-like insoluble organic matter may be  
471 preserved because of kinetics. Insoluble organic matter should start to evolve at temperatures  
472 above  $\sim 125$  °C, which is expected in Ceres' mantle if the latter is compact (Castillo-Rogez et al.  
473 2019). As the temperature of an aqueous system approaches the critical temperature for water,  
474 increased solubility of organic compounds and thermodynamic laws may lead to greater reactivity.

475 This process is consistent with observations of long-lived terrestrial fluids. Fracture fluids from  
476 the Kidd Creek mine in Canada, which have been dated to 2.6 Ga (Holland et al., 2013), may  
477 represent the best terrestrial analog for abiotic carbon chemistry in long-lived liquid reservoirs.  
478 Sherwood Lollar et al. (2021) identified three unique characteristics for Kidd Creek fluids in  
479 comparison to other terrestrial fluids: high concentrations of formate and acetate, acetate/formate  
480 molar ratios  $> 1$ , and  $^{13}\text{C}$  enrichments of acetate. They attributed these characteristics to abiotic  
481 organic synthesis, including both mineral catalysis and radiolytic production, and suggest that the  
482  $^{13}\text{C}$  enrichment may be linked to a dissolved inorganic carbon source. In particular, they noted that  
483 the shorter residence times and lower acetate and formate concentrations reported at  
484 Witwatersrand Basin (Kieft et al., 2018; Onstott et al., 2006a,b) and the longer residence times and  
485 higher concentrations of acetate and formate at Kidd Creek are consistent with experimental  
486 radiolytic production rates for formate and acetate from carbonate and/or bicarbonate ions derived

487 from dissolution of carbonates (Costagliola et al., 2017). Thus, radioactive decay of U, Th, and/or  
488 K may drive carbon chemistry away from thermodynamically stable carbonates towards organic  
489 acids. Such a scenario may ideally represent aging of carbon phases in aqueous systems.

490 Radiolysis may drive the environmental conditions towards more reducing conditions that  
491 eventually favor CH<sub>4</sub> production. Modeling of H<sub>2</sub> production suggests that for an intermediate-  
492 sized body like Ceres, radiolysis may contribute significantly to H<sub>2</sub> (Bouquet et al., 2017). While  
493 it has been suggested that the reduction of CO<sub>2</sub> to CH<sub>4</sub> may be kinetically inhibited in conditions  
494 relevant to Ceres (McKinnon, personal communication), the low H<sub>2</sub>/CH<sub>4</sub> ratio of Kidd Creek fluids  
495 may provide evidence for formation of CH<sub>4</sub> in long-lived natural systems, perhaps via mineral  
496 catalysts (Sherwood Lollar et al., 2002; Reeves and Fiebig, 2020). Such considerations have  
497 previously been used to distinguish between modern and ancient formation of H<sub>2</sub> at Enceladus  
498 (Waite et al., 2017). The rate of radiolysis would be highest early in solar system history; however,  
499 the long half-lives of U and Th especially would lead to continued, significant radioactivity into  
500 the present era. Equilibrium speciation suggests U and Th remain in mineral phases under plausible  
501 ocean world conditions (Neveu et al., 2017), while K may leach into aqueous phases.  
502 Hydrothermal models of Ceres interior predicted serpentinization may cease within 2 to 3 Myr,  
503 but that radiogenic heating would maintain a mud mantle slurry with intimately intermixed mineral  
504 and fluid phases (e.g., Travis et al. 2018).

505 On Ceres, analyzing the detailed brine composition and searching for organic compounds  
506 embedded in the evaporites would help assess the state of the organic matter in Ceres' crust and  
507 residual ocean. The understanding of the co-relationship of salts and organic compounds upon  
508 freezing in conditions relevant to planetary bodies (e.g., potential flash freezing on an airless  
509 surface) is limited by lack of experimental work and relevant terrestrial analogs, although work in  
510 this area is expanding (Thomas et al., 2019; Buffo et al., 2020; Fox-Powell et al., 2021). In  
511 particular, two examples of extraterrestrial halite clasts have been found in the meteorite  
512 collections (Rubin et al., 2002) whose study has revealed various types of organic compounds on  
513 a scale of a few nanometers (Chan et al., 2018). Although the origin of these clasts is unknown,  
514 they are likely representative of the evaporite material found at Ceres (e.g., Fries et al., 2014).

515 **Role of impacts in enabling subsurface-surface material transfer**

516 Fractures created by large impacts on Ceres' surface could tap shallow fluid pockets in the crust,  
517 as has been suggested in the case of Occator crater (Quick et al., 2019; Raymond et al., 2020).  
518 More generally, evidence for old evaporites has been found in association with floor fractures at  
519 large craters such as Dantu (Stephan et al., 2018). Hence, it is likely that large impacts helped open  
520 pathways between the deep interior and the surface throughout Ceres' history. Domes found across  
521 the surface further indicate that volcanic or intrusive activity could have been a widespread process  
522 in space and time (Sori et al., 2018), but whether impact-induced fractures enabled that process is  
523 unknown. Davison et al. (2015) suggested that larger, basin-forming impacts could potentially  
524 excavate Ceres' upper mantle, which could potentially lead to regional-scale distribution of mantle  
525 material (Marchi et al., 2016).

526 Transfer of material in Ceres is expected to be unilateral, helped by the fact that the residual brine  
527 layer or reservoir is likely under pressure (e.g., Neveu and Desch, 2015). On the other hand,  
528 impactors could have contributed new material to the crust. Indeed, recent studies emphasized that  
529 an icy crust can retain a large fraction of impactor material. Bowling et al. (2019) modeled that up  
530 to 70wt.% of impactor material could be embedded in the melt chamber created by the impact-  
531 produced heat. Similarly, Marchi et al. (2018) showed that a large fraction of impactor material  
532 would accumulate in Ceres' outer 5-10 km.

533 In summary, impacts can facilitate material transfer and introduce new material into the crust. As  
534 shown in the case of Occator crater, impacts energetic enough to create fractures that reach below  
535 the crust can lead to the mixing of brine material with impact melt in the shallow subsurface. This  
536 situation can introduce geochemical gradients in the crust. The redistribution of impact-induced or  
537 residual deep and crustal brines can be driven by the thermal alteration of the surface after impact,  
538 driving brines through the subsurface and towards the surface through a combination of  
539 hydrologic, topographic, and material gradients (Schmidt et al., 2020), which is common in  
540 terrestrial environments with freezing or frozen ground. Similar cryo-hydrologic and hydraulic  
541 formation of surface features, including shallow brine zones, has been proposed for Europa  
542 (Schmidt et al., 2011; Schmidt, 2020) and may be relevant for Ceres (where it could be investigated  
543 in relative detail) and other ocean worlds. Since the freezing of brines can chemically fractionate  
544 this potential mixture of initial and impactor material (e.g., Buffo et al., 2020; Buffo et al., 2021,  
545 Fox-Powell et al., 2021), much about drivers of chemical evolution in crustal water solutions could

546 be learned from geophysical probing of the region below Occator crater. Such probing includes  
547 visualization of its fracture network and the geometry of the residual impact melt chamber using  
548 radar techniques and electromagnetic sounding (Grimm et al., submitted).

549

550

## 551 **3.2 Other Ceres Science Themes**

### 552 **Early Solar System History and Dynamical Evolution**

553 The widespread occurrence of ammoniated phyllosilicates and salts and carbon on the surface of  
554 Ceres suggests that Ceres must have formed in a region of the Solar System where primordial  
555 thermodynamic conditions allowed it to effectively retain large amounts of nitrogen and carbon.  
556 Places of formation located in the main asteroid belt, in the interplanetary disk between the orbits  
557 of Jupiter and Neptune, or in the Kuiper belt located beyond the orbit of Neptune, can be  
558 considered, assuming that Ceres (or the materials from which Ceres formed) then migrated from  
559 those regions up to today's position.

560 While the Jupiter-Saturn region has been proposed as the source of most C-type (carbonaceous  
561 and hydrated) asteroids and may represent Ceres' most likely formation region (e.g., Raymond  
562 and Izidoro, 2017; Raymond and Nesvorny, 2020), in recent times the possibility has materialized  
563 that the core of Jupiter itself may have formed further from the Sun and then migrated inward,  
564 dragging with it a multitude of minor bodies (Bosman et al., 2019). The overabundance of  
565 elemental nitrogen measured in Jupiter's atmosphere with respect to the protosolar value (Atreya  
566 et al., 2018) implies that the planet's core must have formed outside or just inside the N<sub>2</sub> ice line  
567 (Öberg and Wordsworth, 2019; Bosman et al., 2019). The position of the latter is difficult to  
568 quantify in the primordial Solar System, but it is of the order of a few tens of AU, which moreover  
569 would point toward a pebble accretion or gravitational instability origin for Jupiter (Bosman et al.,  
570 2019). Alternatively, of amorphous ice with adsorbed volatiles [may have drifted inward](#) to enrich  
571 the gaseous phase of the protosolar nebula with elements such as N, once this ice complex crosses  
572 the amorphous ice snowline, that is the amorphous-to-crystalline ice transition zone.

573 The rapid formation of Jupiter likely destabilized the orbits of nearby planetesimals. Under the  
574 action of the aerodynamic drag due to nebular gas, a fraction of planetesimals was deposited onto  
575 stable orbits inside Jupiter. This process is effective in populating the main outer belt with C-type  
576 asteroids that originated from a large region (5-20 AU) of the disk (Raymond and Izidoro, 2017).  
577 However, this scenario implies that we should find many other small bodies in the asteroid belt  
578 with a composition similar to Ceres, whereas Ceres' bulk composition is atypical compared to C-  
579 type asteroids. An explanation for this apparent paradox may be that Ceres may have undergone a  
580 certain degree of pebble accretion before being scattered inwards. Because the efficiency of this  
581 process is directly proportional to the size of planetesimal (Johansen et al., 2015), a primordial  
582 body the size of Ceres could have grown more volatile-rich from pebbles that originated in the  
583 outer solar system than similar bodies of smaller size (Kretke et al., 2017). Alternatively, Ceres  
584 could have started out from the same composition as C-types but now displays a different surface  
585 composition because its physico-chemical evolution was different. (e.g., more prolonged and/or  
586 hotter aqueous alteration, material concentration on the surface).

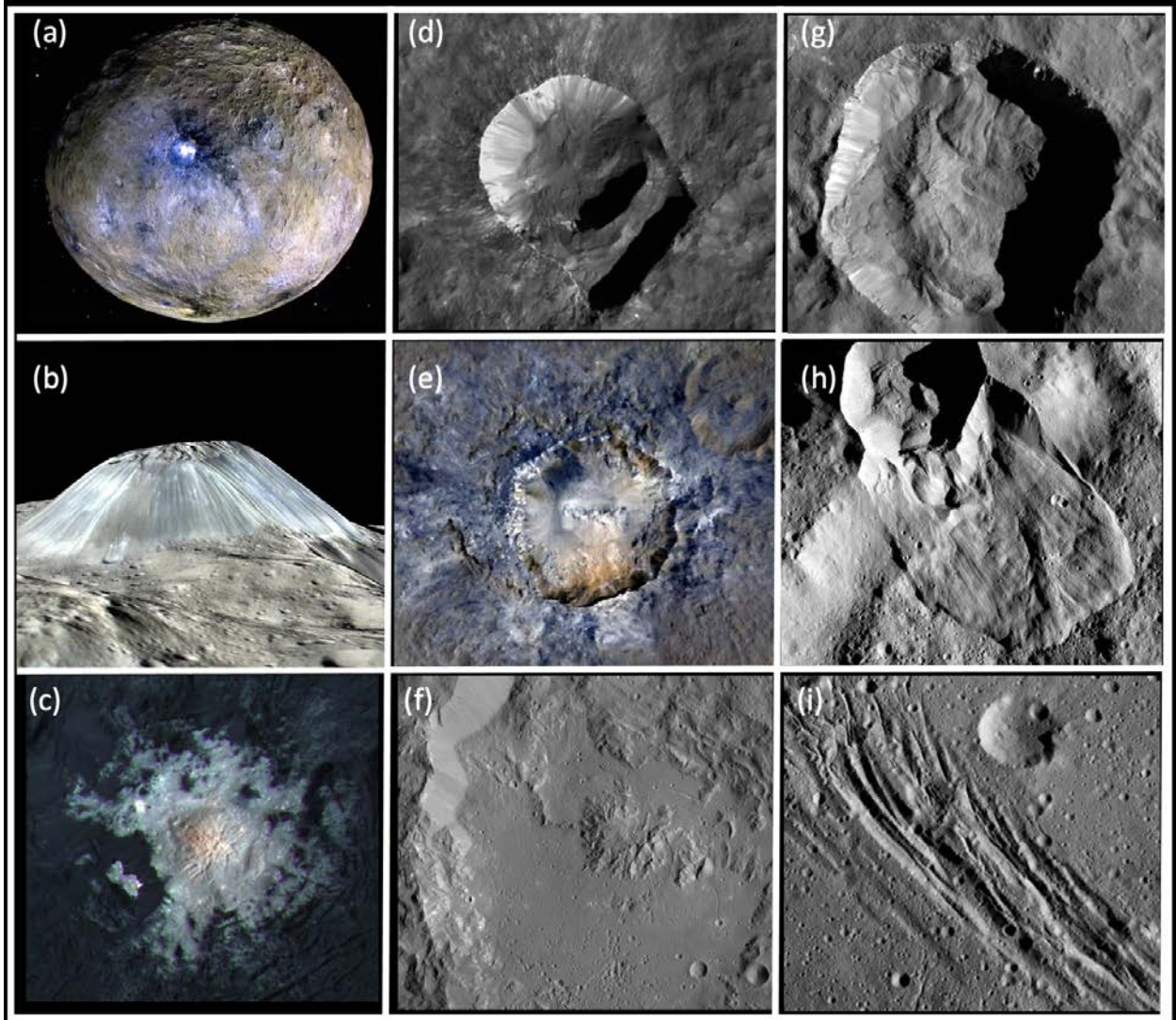
587 A competing origin for the high abundance of ammonia found at Ceres is that it was released from  
588 the metamorphism of organic compounds (McSween et al., 2018). Experimental work by  
589 Pizzarello and Williams (2011) suggests that pressures of tens of megapascals and temperatures  
590 of a few hundred degrees are sufficient to drive organic breakdown on a short timescale. These  
591 conditions are expected to have prevailed in Ceres' mantle for an extended period of time (Castillo-  
592 Rogez and McCord, 2010).

593 In summary, the origin of Ceres is a major open question with fundamental implications about the  
594 origin of volatiles and organic matter in the inner solar system (e.g., Budde et al., 2019), the  
595 mechanisms driving the solar system architecture, and the role that large planetesimals could have  
596 played by impacting the growing planets (e.g., Salmon and Canup, 2019). Castillo-Rogez et al.  
597 (2020) pointed out that analysis of returned material from Ceres in Earth's facilities is the best  
598 approach to resolving the origin of Ceres because the complex and evolving chemical and  
599 dynamical framework describing the early solar system warrant adaptability in the measurements  
600 to be carried out, and because of additional complications specific to dealing with a very large  
601 planetesimal (e.g., pebble accretion, alteration during evolution).

602 **Ceres as a natural laboratory to study geological processes in ice-rich crust**

603 Geological history is well recorded on Ceres relative to resurfaced worlds like Europa. Ceres may  
604 also represent an advanced, less active state of worlds like Europa, and thus represents a major  
605 endmember on the varied spectrum of icy objects. In both ways, Ceres may serve an analogous–  
606 and as important–role in our understanding of icy worlds as the Moon does in our understanding  
607 of terrestrial planets.

608 As a result of Ceres’ special role in our understanding of icy worlds, many icy geological processes  
609 that operate throughout the Solar System would be elucidated by further study at Ceres (Figure 5).  
610 Impact cratering, one of the dominant geological processes in the Solar System, has been shown  
611 to result in similar crater sizes and morphologies on Ceres as on other icy bodies (Hiesinger et al.,  
612 2016; Schenk et al., 2021), and thus Ceres holds promise for more detailed study of impacts into  
613 icy targets. Cryovolcanism has likely been an important process of interior-surface exchange on  
614 a number of icy worlds (e.g., Enceladus, Spencer and Nimmo, 2013), and Ceres provides an  
615 opportunity for further study of its mechanisms and products. Geophysical analysis of icy crustal  
616 structure has been performed on Ceres with more precise data than on any other icy object (Park  
617 et al., 2020), but can be greatly improved upon with future missions. Tectonic processes likely  
618 also occur on Ceres (e.g., Bland et al., 2019; Ruiz et al., 2019) and may elucidate icy tectonics in  
619 general. Geologic processes on Ceres including tectonics, landslides and other material flows  
620 (e.g., Schmidt et al., 2017; Hughson et al., 2019) as well as cryo-hydrologic features (Schmidt et  
621 al., 2020) may involve a mixture of silicates, ice, and water common to glacial environments on  
622 the Earth and Mars, and thus represent another opportunity to explore this understudied physical  
623 regime. Additional study of Ceres’ interior structure would inform when and how ice-rich bodies  
624 differentiate, a process with major implications for planetary evolution. Finally, analysis of the  
625 Dawn data raised the question of the level of exogenic inputs to the surface and shallow subsurface  
626 of water-rich airless bodies (Vernazza et al. 2017; Marchi et al. 2018). This topic is critical because  
627 the introduction of exogenic material into the crust, especially if it also involves impact melt,  
628 carries the potential to significantly alter the crustal composition (Bottke et al., 2013). In many  
629 ways, Ceres thus provides an accessible natural laboratory for understanding icy geological  
630 processes.



631

632 *Figure 5. Examples of landforms found at Ceres that make it a natural laboratory to study geological*  
 633 *processes in ice-rich crust. Left column: Expressions of brine-driven activity: (a) recent evaporite exposure*  
 634 *in Occator crater; (b) Ahuna Mons, a volcano built with rock and brine (Ruesch et al., 2016, 2019a); (c) close-*  
 635 *up view of Cerealia Facula. Cerealia Tholus in the center displays evidence of hydrohalite at its top (here*  
 636 *appearing in light pink in this enhanced color version, De Sanctis et al., 2020). Middle column: influence of*  
 637 *ice on crater properties: (d) direct exposure of ice at Oxo crater (Combe et al., 2016); (e) fresh salt-rich ejecta*  
 638 *and central crest in Haulani crater (Tosi et al., 2018); (f) flat floor resulting from impact-generated heat and*  
 639 *melting in Ikapati crater. Right column: other ice-driven landforms found on Ceres' surface: (g) glacier-like*  
 640 *features in Juling crater (Raponi et al., 2018); (h) landslide whose morphology indicates a high ice content*  
 641 *(Schmidt et al., 2016); (i) Normal faulting in an ice rich crust at Nar Sulcus in Yalode crater (Hughson et al.,*

642 2018). Credit: NASA/JPL-Caltech/UCLA/MPS/DLR/IDA, based on PIA22090 that contains details information  
643 on the origin of these pictures.

#### 644 **Ceres as a natural laboratory for understanding processes affecting airless bodies**

645 Transient atmospheres and exospheres of airless bodies are known on Mercury, the Moon, and  
646 some icy moons of the outer solar system. These are caused either by an interaction of the space  
647 environment (meteorites, radiation) with the surface or by endogenic processes. Thus, a systematic  
648 study of these phenomena can reveal important clues on the nature of surfaces and subsurface  
649 geologic processes.

650 Water ice sublimation due to solar irradiation and solar wind particle bombardment are possible  
651 mechanisms for Ceres' weak exosphere (e.g., Landis et al., 2018). Some of the released water  
652 molecules can be re-trapped in permanently shadowed polar depressions, leading to thin ice  
653 deposits (Schorghofer et al., 2016; Platz et al., 2017). In addition, endogenic sources of various  
654 molecules (H<sub>2</sub>O, CH<sub>4</sub>, CO<sub>2</sub>) are conceivable (Nathues et al., 2017). Cryovolcanic processes, as  
655 suggested for Occator crater (e.g., Nathues et al., 2020), could be responsible for the development  
656 of a transient exosphere composed of different molecules and particles. Thus, Ceres is expected to  
657 be an ideal target to characterize the exosphere or transient atmosphere of an airless body.  
658 However, the search for these features has proved difficult. While a thin OH exosphere was  
659 concluded from observations of the International Ultraviolet Explorer by A'Hearn and Feldman  
660 (1992), other studies using ground-based and space-based telescopic data could not confirm its  
661 existence (Rousselot et al., 2011; Roth et al., 2016, 2018). Kueppers et al. (2014) reported  
662 occasional water vapor from spectral data of the Herschel space observatory. Further evidence of  
663 a transient cerean atmosphere was derived from observations of Dawn's Gamma Ray and Neutron  
664 Detector upon arrival at Ceres (Villarreal et al., 2017), likely correlated with solar activity.  
665 However, since the Dawn payload was not designed to detect an exosphere or a thin atmosphere,  
666 their density and composition are until today largely unexplored.

667 Exposed water ice, which could be a possible source for an exosphere, was detected at several sites  
668 (Combe et al., 2016, 2018); even a seasonal variation of ice exposure in the Juling crater has been  
669 reported by Raponi et al. (2018). In addition, high phase angle imaging with the Dawn Framing  
670 Camera revealed an unusual light scattering behavior associated with the Occator faculae. This

671 unique light scattering was attributed to an additional component to the solid surface, i.e., an  
672 optically thin and near-surface haze layer (Nathues et al., 2015, 2019; Thangjam et al., 2016). The  
673 hydrohalite detected by De Sanctis et al. (2020) at Occator tholus is a possible source for the  
674 ongoing production of water and haze. The database on exospheric observable effects, events, and  
675 sources at Ceres is still sparse and requires follow-on observations to derive radial density  
676 distribution, composition, and flux rates.

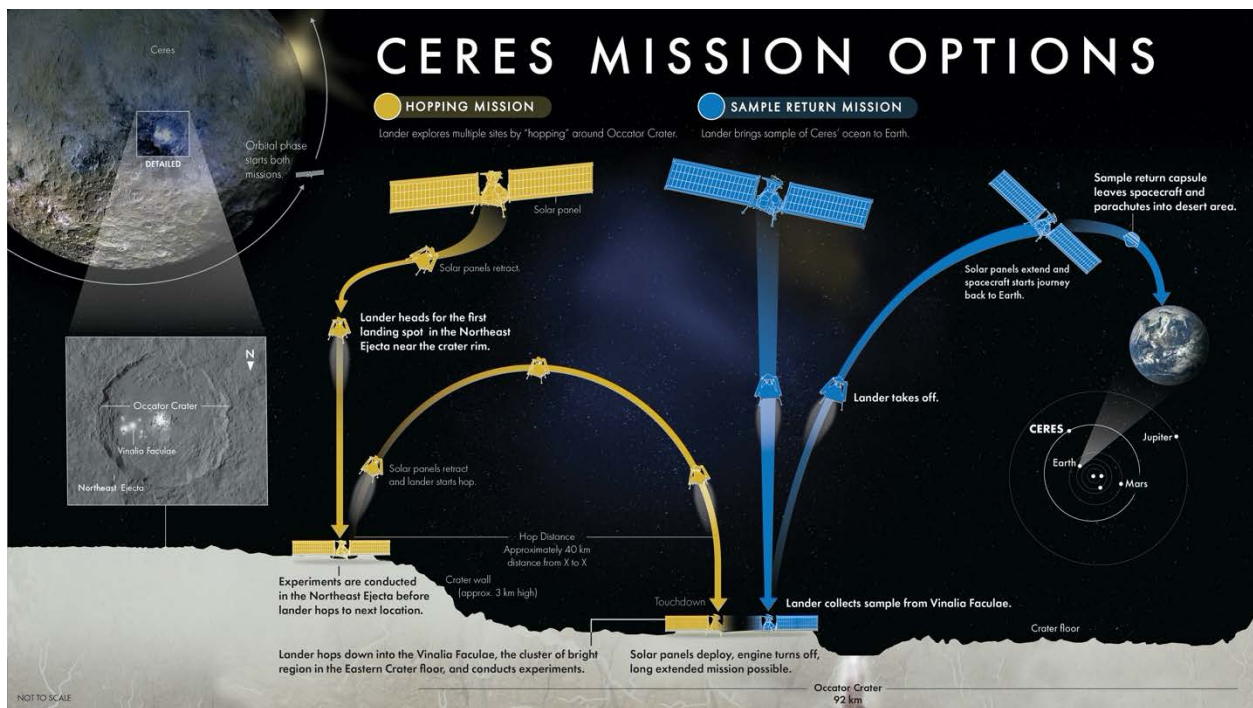
## 677 **4. Approaches to the Future Exploration of Ceres**

678 This section addresses approaches to further the exploration of Ceres, with future spacecraft but  
679 also via theoretical and experimental research, field work at terrestrial analogs, and Earth-based  
680 observations.

### 681 **4.1 Future Missions**

682 A future mission to Ceres could address open questions about Ceres' past and current habitability  
683 potential and address some of the aforementioned processes in greater depth. Direct surface access  
684 of material evolved from the deep brines provides a unique opportunity to investigate the evolution  
685 of long-lived oceans. A recent study developed under NASA's Planetary Mission Concept Study  
686 (PMCS) program showed that significant progress in our understanding of Ceres as an evolved  
687 ocean world requires resources offered by NASA's *New Frontiers* and *Flagship* programs  
688 (Castillo-Rogez et al., submitted). The PMCS study identified two mission architectures that can  
689 address a majority of the science questions listed above under a *New Frontiers* cost cap: a sample  
690 return from an evaporite-rich site in Occator crater, or a hopper that explores the evaporites and an  
691 additional site (Figure 6). Both concepts include an orbital phase for landing site selection and  
692 certification prior to high-precision landing. For little additional cost, the orbiter can accommodate  
693 high-resolution imaging and gravity measurements at a handful of sites of interest to address past  
694 and current activity. Landed investigations are required for interior probing and compositional  
695 analysis either via sample return or using a combination of instruments for elemental,  
696 mineralogical, and isotopic measurements of evaporites and floor (non-evaporite) material.  
697 Electromagnetic sounding was identified as the most promising approach for probing Ceres'  
698 interior for deep brine distribution (Grimm et al., in press).

699 Ceres' low gravity renders wheeled platforms mostly impractical but a lander can access multiple  
 700 sites on Ceres via thruster-assisted hopping (Figure 5). The number and separation of sites that  
 701 may be reached depend on mass budget and risk posture. Scully et al. (accepted) demonstrated  
 702 that many potential landing sites are available in the regions of interest based on the best resolution  
 703 data returned by the Dawn mission. Furthermore, that study assessed the accessibility of sites at  
 704 Haulani craters and Ahuna Mons, which are also of scientific interest: Haulani's ejecta are  
 705 excavated from the shallow crust, which records the conditions in Ceres' early ocean, whereas a  
 706 greater understanding of Ahuna Mons' composition, flank structure, and subsurface structure  
 707 would help narrow down the mechanism driving the transfer of material from the upper mantle  
 708 brine region to the surface.



709  
 710 *Figure 6. Two architectures proposed for addressing key open questions about Ceres' endogenic activity,*  
 711 *habitability potential, and origin. The in situ architecture is a hopper that explores two sites at Occator crater,*  
 712 *the first one at the northeastern ejecta blanket called Homowo Regio and the second one in the Vinalia*  
 713 *Faculae. The second concept would return a sample from the Vinalia Faculae. Both concepts would include*  
 714 *an orbital phase during which high-resolution imaging and gravity data are acquired at key landforms of*  
 715 *potential cryovolcanic origin. Also, in both concepts, the in situ phase includes an electromagnetic*  
 716 *investigation that would map the distribution of brines below Occator crater, down to 50 km depth (Castillo-*  
 717 *Rogez et al., submitted). Credit: Raoul Ranoa.*

718

719 **Required Technologies for Future Missions to Ceres:** Few new technologies are required for a  
720 future in situ or sample return mission at Ceres. An important one identified by the Ceres PMCS  
721 is the certification of existing retractable solar arrays in Ceres-relevant environments. Other  
722 required technologies already leverage investments for previous projects, e.g., terrain relative  
723 navigation (Mars 2020) and throttleable descent engines (Europa Lander pre-project).

## 724 **4.2. Supporting Activities**

725 The list of activities below needed to progress with our understanding of Ceres and prepare for  
726 future exploration is not exhaustive but illustrates possible pathways.

727 *Data Analysis:* In order to increase the science return from the Dawn mission and prepare for a  
728 follow-on mission to Ceres, we recommend continuous support to the following areas; (1) Data  
729 Analysis Programs would support a vast array of investigations by the broad community that build  
730 on, revisit, and expand upon previous analyses of the Dawn data; (2) High-quality geologic map(s)  
731 of regions of interest for future landed missions would be integral to planning future observations  
732 for landing site reconnaissance and selection; (3) Comparative analysis of the morphologies of  
733 ejecta deposits, debris flows, structures, and constructional features on Earth, Mars, Ceres, and icy  
734 moons.

735 *Theoretical and Experimental Research:* Future exploration of Ceres would benefit from work on  
736 terrestrial and laboratory analogs with a focus on better understanding the physics and chemistry  
737 of brines, organic matter, and mud mixtures in mid-size bodies, which are emerging topic of  
738 importance to ocean worlds. Specific support for the following studies is recommended.  
739 Laboratory research on salt clasts present in meteorite collections, which have been suggested to  
740 come from Ceres or a Ceres-like body (e.g., Chan et al. 2018); thermophysical properties of brines,  
741 hydrated salts, and clathrates; mechanical response of evaporites to impacts, a key input to deriving  
742 the faculae model ages based on crater counts, which is key to many science drivers; effect of  
743 radiolysis in the creation of redox gradients in ocean worlds, for example, to understand the  
744 efficiency of this process and its potential to create local habitable zones; irradiation processes  
745 (ion, UV) that modify the infrared signatures of minerals and organic compounds; behavior of  
746 brine and mud mixtures in zero-pressure surface environments at Ceres temperatures, e.g., flow

747 properties such as fluid-rich debris flows and impact ejecta; devolatilization process of the  
748 evaporites in a vacuum for water budget and evaporite deposit age estimates; experimental  
749 simulation of brine/organic/mud convection to inform the understanding of thermal evolution and  
750 material transfer in the interiors of mid-sized icy bodies; synthesis and characterization of analog  
751 materials to provide comparison datasets at appropriate conditions for Ceres' surface, and to  
752 support the definition and development of new instruments, e.g., to investigate organic carbon in  
753 mud and/or salt mixtures.

754 *Work on Terrestrial Analog Sites:* Geomorphological and first-order geochemical analog sites for  
755 regions of interest on Ceres exist throughout the solar system, especially on the Earth and Mars.  
756 Of specific interest are soda lakes (Castillo-Rogez et al., 2020), hydrothermal systems, landslide  
757 and ejecta deposits, salt domes and other salt tectonics structures, and periglacial features such as  
758 rock glaciers, protalus lobes, and pingos (Schmidt et al., 2017, 2020). Potential analog sites on  
759 Earth can be used for testing relevant planetary instruments, surveying strategies, and sampling  
760 systems required for future missions to Ceres. This is particularly relevant for landed assets where  
761 little is currently known about the sub-meter scale geology and physical properties of the surface.

762 Periglacial environments on Earth are also scientifically interesting analogs for various locations  
763 on Ceres because of its inferred subsurface ice content (e.g., Prettyman et al., 2017) and myriad  
764 surface features whose morphologies suggest an icy origin (e.g., Schmidt et al., 2017, 2020;  
765 Hughson et al., 2019). Beyond magnetotelluric sounding identified in the PMCS to investigate  
766 Ceres' deep subsurface (Grimm et al., submitted), techniques such as ground penetrating radar,  
767 frequency- and time-domain electromagnetic sounding could further reveal Ceres' shallow  
768 stratigraphy. Deploying these techniques in analog periglacial environments would enhance the  
769 interpretation of future electromagnetic geophysical results from Ceres (e.g.,  
770 <https://schmidt.eas.gatech.edu/pingo-starr/>). While glaciers and ice sheets have been extensively  
771 subjected to geophysical investigation, more Ceres-like analogs such as protalus lobes, alpine  
772 tundra, and pingo covered landscapes have remained relatively understudied. Understanding how  
773 electromagnetic systems respond in both evaporitic and periglacial environment, as well as a  
774 deeper geophysical understanding of periglacial systems on Earth are critical for preparing for  
775 landed geophysical exploration of Ceres.

776 *Ground-Based Observations:* Telescopic observations from Earth or near-Earth space should  
777 continue, for example to address the following questions: (a) the origin of Ceres' sporadic  
778 outgassing activity with regular (perihelion and seasonal) and reactive observations following the  
779 release of solar energetic protons (Villarreal et al., 2017); (b) additional constraints on Ceres'  
780 surface composition from observations in the ultraviolet (e.g., Hubble Space Telescope) and mid-  
781 infrared wavelengths (e.g., James Webb Space Telescope Mid-InfraRed Instrument), which are  
782 complementary to the 0.4-5  $\mu\text{m}$  range observed by Dawn. The next generation of space telescopes  
783 could also revolutionize the study of Ceres. The Large UV, Optical and InfraRed Surveyor mission  
784 (LUVOIR), a 15 m or 8 m primary space telescope being considered for selection by the 2020  
785 Astrophysics decadal survey, made the case for further spatially resolved imaging (11-20  
786 km/pixel) and spectroscopy (tens of km) of the surface of Ceres. The high spectral resolution of  
787 LUVOIR or similar telescopes across the UV-near IR wavelength range would allow global studies  
788 of Ceres' composition, and searches for outgassing in the UV (LUVOIR Team 2019).

## 789 **5. Conclusions**

790 Ceres is a rich destination that displays evidence for features pertinent to ocean world science,  
791 such as forms of brine-driven effusion, organic matter, geological processes, impact melt, etc. It is  
792 also the large ice-rich object closest to Earth, accessible for in situ exploration and/or sample return  
793 under a *New Frontiers*- or small *Flagship*-class cost cap because of its relative low gravity.  
794 Sampling freshly exposed evaporites would provide insights into the chemical and physical  
795 properties of a long-lived brine reservoir and test hypotheses of interest to ocean worlds, such as  
796 the prospect for the late enrichment of a residual ocean in volatiles released from the mantle and  
797 radiolysis as a long-term chemical energy source. Long-lived activity in Ceres requires processes  
798 or crustal properties that remain to be confirmed but are expected to also apply to other dwarf  
799 planets and icy moons. More generally, Ceres might be the first example of “muddy” ocean world,  
800 a class of bodies that might be frequent among mid-sized icy bodies whose hydrosphere may be  
801 frozen but whose mantle porosity is filled in with brines for an extended period of time. Processes  
802 known to occur in Earth' sediments, such as organic chemistry or radiolysis, are presumably  
803 relevant and their occurrence in Ceres may be tested in future exploration.

804 Per its high content in nitrogen and carbon, Ceres (or at least the materials from which it formed)  
805 is suspected to originate from the outer solar system, although competing hypotheses remain.  
806 Resolving this question is fundamental to firmly anchor our understanding of early solar system  
807 evolution and the origin of water and organics in the inner solar system. Hence, determining Ceres'  
808 origin, the relationship of its volatiles and organics to other inner solar system bodies (icy moons  
809 and other dwarf planets), and implications for solar system dynamical evolution are additional  
810 drivers for the future exploration of Ceres.

811 Several recent mission concepts have independently emphasized science objectives that include a  
812 quantification of Ceres' past and current habitability and use Ceres as a test case for unraveling  
813 the habitability, over time, of volatile-rich bodies. The Ceres Planetary Mission Concept Study  
814 concluded that significant progress along the Roadmap to Ocean Worlds (Hendrix et al., 2019) can  
815 be achieved with in situ exploration, either at multiple sites, or at a single site and with a sample  
816 return. However, only a sample return mission can fully retire questions about Ceres' origin and  
817 the habitability potential of its residual brines. A mission returning a sample from Ceres'  
818 evaporites would address cross-cutting astrobiology goals pertinent to ocean worlds and is also  
819 being recommended by independent groups (Burbine and Greenwood, 2020; Gassot et al., 2020;  
820 Shi et al., submitted).

821 Supporting scientific work, in the form of experimental research on Ceres material analogs,  
822 ground-based telescopic observations, and continued analysis of the Dawn data, is needed to  
823 further increase the science return from the Dawn mission and pave the way for follow-on  
824 exploration. Lastly, a future mission to Ceres that would optimistically kick off in the mid-2020s  
825 and return a sample by 2045 requires the participation of a diverse, inclusive, and thriving  
826 community.

827 **Acknowledgements:** Part of this research was carried out at the Jet Propulsion Laboratory, California Institute of  
828 Technology, under a contract with the National Aeronautics and Space Administration (80NM0018D0004).

## 829 REFERENCES

- 830 A'Hearn, M. F., & Feldman, P. D. (1992). *Icarus*, 98(835)  
831 54–60. [https://doi.org/10.1016/0019-1035\(92\)90206-836](https://doi.org/10.1016/0019-1035(92)90206-836)  
832 Alexander C. M. O'D., Howard K. T., Bowden R., and  
833 Fogel M. L. 2013. *Geochimica et Cosmochimica Acta* 838  
834 123, 244-260. 839  
840 Alexander, C. M. O'D., Bowden R., Fogel M. L., and  
Howard K. T. 2015. *Meteoritics & Planetary Science* 50,  
810-833.  
Alexander, C. M. O'D., et al. (2017) *Chem. Erde -  
Geochem.* 77, 227–256,  
doi:10.1016/j.chemer.2017.01.007.

841 Ammannito, E., DeSanctis, M.C., Ciarniello, M., et al. 884  
842 (2016) *Science* 353, aaf4279. 885  
843 <https://doi.org/10.1126/science.aaf4279> 886

844 Atreya, S.K., Crida, A., Guillot, T., et al. In: *Saturn 887*  
845 the 21st Century, ed. K. Baines et al. (Cambridge 888  
846 Cambridge Univ. Press), 5 (2018). Doi: 889  
847 [10.1017/9781316227220.002](https://doi.org/10.1017/9781316227220.002). 890

848 Bierson, C.J., Nimmo, F. and Stern, S.A. (2020) *Nature*  
849 *Geoscience* 13, 468-472. 891

850 Bland, M.T., Raymond, C.A., Schenk, P.M., et al., 892  
851 2016. *Nature Geosci* 9, 538–542. 893  
852 <https://doi.org/10.1038/ngeo2743> 894

853 Bland, M.T., et al. (2019) *Nature Geosciences* 12, 797-  
854 801 895

855 Bosman, A.D., Cridland, A.J., Miguel, Y. *A&A* 632,  
856 L11 (2019). Doi: [10.1051/0004-6361/201936827](https://doi.org/10.1051/0004-6361/201936827). 898

857 Bottke, W.F., Vokrouhlický, D., Nesvorný, D. and  
858 Moore, J.M. (2013) *Icarus* 223, 775-795 899  
859 <https://doi.org/10.1016/j.icarus.2013.01.008> 900

860 Bouquet, A., Glein, C.R., Wyrick, D. and Waite, J.H.,  
861 2017. *The Astrophysical Journal Letters* 840, L803  
862 <https://doi.org/10.3847/2041-8213/aa6d56> 904

863 Bowling, T.J., Ciesla, F.J., Davison, T.M., et al. (2019)  
864 *Icarus* 320, 110-118. 905

865 Brearley A. J., 2006. In *Meteorites and the Early Solar*  
866 *System II*, editors Lauretta D. S. and McSween H. Y., pp.  
867 587-624, University of Arizona Press. 908

868 Brown, M., Hand, K. (2013), *Astronom. J.* 145. 909

869 Browning L. B., McSween H. Y., and Zolensky M. E.,  
870 1996. *Geochimica et Cosmochimica Acta* 60, 2627-  
871 2633. 910

872 Buczkowski, D. L., et al. (2016) *Science* 353, id.aaf4332  
873 Buczkowski, D. L., et al. (2018) *JGR* 123, 3188-3204 915  
874 Budde+ (2019) *Nature Astron.* 3, 736-741. 916

875 Buffo, J. J., B.E. Schmidt, C. Huber, C. C. Walker  
876 (2020) *JGR Planets*. 918  
877 <https://doi.org/10.1029/2020JE006394> 919

878 Buffo, J. J., Meyer, C. R., Parkinson, J.R.G, (2021) In  
879 revision, *JGR: Planets*, posted online at ESOARXIV  
880 <https://doi.org/10.1002/essoar.10504589.1> 921

881 Burbine, T., Greenwood, R. (2020) *SSR* 216:59. 922

882 Carrozzo, F. G., et al. (2018) *Science Advances* 4,  
883 e1701645. 923

Castillo-Rogez J. C. and McCord T.B., 2010. *Icarus* 205,  
443-459. 924

Castillo-Rogez, J., Neveu, M., McSween, H.Y., et al.  
(2018) *Meteoritics & Planetary Science* 53, 1820–  
1843. <https://doi.org/10.1111/maps.13181> 925

Castillo-Rogez, J. C., et al. (2019) *Geophys. Res. Lett.*  
46, 1963-1972. 926

Castillo-Rogez, J. C. (2020) *Nature Astron.* 4, 732-734.

Castillo-Rogez, J. C., et al. (2020) *Astrobiology*, Feb  
2020.269-291.

Castillo-Rogez, J. C., et al. submitted to *The Planetary  
Science Journal*, in revisions.

Castillo-Rogez and Bland (2021) Cambridge University  
Press, in press.

Chan, Q., et al. (2018) *Science Advances* 2018;4:  
eaao3521.

Combe, J.-P., McCord, T.B., Tosi, F., et al. (2016)  
*Science* 353, aaf3010.  
<https://doi.org/10.1126/science.aaf3010>

Combe, J.-P., Raponi, A., Tosi, F., et al. (2018) *Icarus*,  
318, 22–41.  
<https://doi.org/10.1016/j.icarus.2017.12.008>

Costagliola, A., Vandenborre, J., Blain, G., et al. 2017.  
*The Journal of Physical Chemistry C* 121, 24548-24556.  
<https://doi.org/10.1021/acs.jpcc.7b07299>

Danger, G., Ruf, A., Maillard, J., et al. 2020, *Planet Sci  
J*, 1, 55,  
<https://iopscience.iop.org/article/10.3847/PSJ/abb60f>

Davison et al. (2015) 46th Lunar and Planetary Science  
Conference, LPI contrib. no. 1832, p.2116.

De Sanctis, M.C., Ammannito, E., Raponi, A., et al.  
(2015) *Nature* 528, 241–244.  
<https://doi.org/10.1038/nature16172>

De Sanctis, M.C., Raponi, A., Ammannito, E., et al.  
(2016) *Nature* 536, 54–57.  
<https://doi.org/10.1038/nature18290>

De Sanctis, M. C., et al. (2017) *Science* 355, 719-722.

De Sanctis, M. C., et al. (2019) *MNRAS* 482 2407–2421,  
<https://doi.org/10.1093/mnras/sty2772>

De Sanctis, M. C., Ammannito, E., Raponi, A., et al.  
(2020) *Nat Astron* 4, 786–793.  
<https://doi.org/10.1038/s41550-020-1138-8>

Denton+ (2021) *Geophys. Res. Lett.* 48.

927 Desch, S., Neveu, M. (2017) *Icarus* 287, 175-186. 969

928 Ermakov, A., et al. (2017) *Journal of Geophysical Research* 122, 2267–2293. 970

929 971

930 Fagents, S. A. (2003) *Journal of Geophysical Research* 108, 5139. 972

931 973

932 Formisano, M., et al. (2018) *JGR* 123, 2445-2463. 974

933 Formisano, M., Federico, C., Castillo-Rogez, J., De Sanctis, M.C. and Magni, G. (2020) *Monthly Notices of the Royal Astronomical Society* 494(4), 5704-5712. 975

934 976

935 977

936 Fortes, A. D. (2007) *Icarus* 191, 743-748. 978

937 Fox-Powell, M., Cousins, C. R. (2020) *J. Geophys. Res. Planets* 126, ee2020JE006628 979

938 980

939 Fries, M., et al. (2014) Workshop on the Habitability of Icy Worlds, held 5-7 February, 2014 in Pasadena, California. LPI Contribution No. 1774, p.4078. 981

940 982

941 983

942 Fu, R. R., et al. (2017) The interior structure of Ceres revealed by surface topography, *EPSL* 476, 153-164. 984

943 985

944 Gassot et al. 2020 *Acta Astronautica* <https://doi.org/10.1016/j.actaastro.2020.12.050>. 986

945 987

946 Gil-lozano 2020 *Scientific report*, DOI: 10.1038/s41598-020-71657-9 988

947 989

948 Glavin, D. P., Callahan, M. P., Dworkin, J. P., Elsila, E. (2010) *MaPS* 45, 1948–1972. doi:10.1111/j.1945-5100.2010.01132.x 990

949 991

950 992

951 Grimm, R., et al., Submitted to *Icarus*. 993

952 Haas et al, 2020, *Communication Chemistry* doi.org/10.1038/s42004-020-00387-w 994

953 995

954 Hamilton V. E., Goodrich C. A., Treiman A. H., et al. (2020) *Nature Astronomy*, doi.org/10.1038/s41550-020-01274-z. 996

955 997

956 1000

957 Hendrix, A. R., et al. (2019) The NASA Roadmap for Ocean Worlds, *Astrobiology*, 19:1. 1001

958 1002

959 Hesse, M. A., Castillo-Rogez, J. C. (2019) *Geophysical Research Letters* doi.org/10.1029/2018GL080327 1003

960 1004

961 Hiesinger, H., et al. (2016), *Science* 353, aaf4759 1005

962 doi:10.1126/science.aaf4759 1006

963 Holland, G., Sherwood Lollar, B., Li, L., et al., 2013. 1007

964 *Nature* 497, 357-360 1008

965 <https://doi.org/10.1038/nature12127> 1009

966 Howard K. T., Benedix G. K., Bland P. A., and Crespey G. 2011. *Geochimica et Cosmochimica Acta* 75, 2735-2751. 1010

967 1011

968 1011

Howard K. T., Alexander C. M. O'D., Schrader D. L., and Dyl K. A. 2015. *Geochimica et Cosmochimica Acta* 149, 206-222.

Hughson, K. H. G., Russell, C. T., Schmidt, B. E., et al. (2018) *Geophys. Res. Lett.* 46, 80-88.

Hughson, K. H. G., Russell, C. T., Schmidt, B. E., et al. (2019). *JGR Planets*. <https://doi.org/10.1029/2018JE005666>

Hussmann, H., Sohl, F. and Spohn, T. (2006) *Icarus* 185, 258-273

Johansen, A., Mac Low, M.-M., Lacerda, P., Bizzarro, M. *Science Advances* 1 (3), id. 1500109 (2015). Doi: [10.1126/sciadv.1500109](https://doi.org/10.1126/sciadv.1500109).

Johnson and Sori (2020) *J. Geophys. Res. Planets* 125.

Kamata, S., Nimmo, F., Sekine, Y., et al. (2019) *Nature Geoscience* 12, 407-410.

Kaplan, H., et al. (2018) *Geophys. Res. Lett.* 2018, 45, 5274–5282, doi:10.1029/2018GL077913.

Keane, J.T., Matsuyama, I., Kamata, S. and Steckloff, J.K. (2016) *Nature* 540, 90-93.

Kebukawa, Y., Kilcoyne, D., Cody, G. (2013) *ApJ* 771 19.

Kebukawa, Y., et al, 2020 *Icarus* 347.

Kerridge, J. F. (1999) In: *Composition and Origin of Cometary Materials*, Eds. K. Altwegg, P. et al., *Space Science Series of ISSI* 8, Springer, 275-288.

Kieft, T.L., Walters, C.C., Higgins, M.B., et al. (2018) *Organic geochemistry* 118, 116-131. <https://doi.org/10.1016/j.orggeochem.2018.02.003>

Kranck, K. (1973) *Nature* 246, 348-350.

Kretke, K.A., Bottke, W.F., Levison, H.F., et al. (2017) *Accretion: Building New Worlds Conference*, Proceedings of the conference held 15-18 August, 2017 in Houston, Texas. LPI Contribution No. 2043, id.2027. <https://www.hou.usra.edu/meetings/accretion2017/pdf/2027.pdf>.

Krohn, K., et al. (2016) *GRL* 43, 11,994-12,003.

Krohn, K., et al. (2018) *GRL* 45, 8121-8128.

Krohn, K., et al. (2020) *PSS* 187, id. 104955.

Küppers, M., O'Rourke, L., Bockelée-Morvan, D., et al. (2014) *Nature*, 505(7484), 525–527. <https://doi.org/10.1038/nature12918>

Landis, M., et al. (2017) *JGR* 122, 1984-1995.

1012 Landis, M. E., Byrne, S., Combe, J.-P., et al. (2015) *Journal of Geophysical Research: Planets*, 124, 61–1054  
1013 <https://doi.org/10.1029/2018JE005780>  
1014  
1015 Le Guillou, C., et al. (2014) *Geochimica et Cosmochimica Acta* 131, 368–392.  
1016  
1017 Lunine, J. I., Stevenson, D. (1985) *AJ Suppl. Series* 58, 493-531.  
1018  
1019 Lunine, J. I., Stevenson, D. (1987) *Icarus* 70, 61-77.  
1020  
1021 LUVUOIR Team, 2019. The LUVUOIR mission concept study final report. arXiv preprint arXiv:1912.06219.  
1022  
1023 Marchi, S., et al. (2016) *Nature Comm.* 7, 12257.  
1024  
1025 Marchi, S., et al. (2019) *Nature Astron.* 3, 140-145.  
1026  
1027 Mao X., McKinnon W. B., 2018. *Icarus* 299, 430-442.  
1028  
1029 Matthewman, R., Martins, Z. and Sephton, M.A., 2011. *Astrobiology* 13, 324-330.  
1030 <https://doi.org/10.1089/ast.2012.0820>  
1031  
1032 McCord, T.B., Sotin, C., 2005. Ceres: Evolution and current state. *J. Geophys. Res.* 110, E05009.  
1033 <https://doi.org/10.1029/2004JE002244>  
1034  
1035 McSween H., Emery J.P., Rivkin A.S., et al. (2010) *Meteoritics & Planetary Science* 53, 1793-1804.  
1036  
1037 Melwani Daswani *et al.*, submitted to *Geophys. Res. Lett.*  
1038  
1039 Mousis, O., Ronnet, T., Lunine, J.I. The Astrophysical Journal, 875:9. Doi: [10.3847/1538-4357/ab0a72](https://doi.org/10.3847/1538-4357/ab0a72).  
1040  
1041 Nathues, A., Hoffmann, M., Schaefer, M. et al. *Nature* 528, 237–240 (2015).  
1042 <https://doi.org/10.1038/nature15754>  
1043  
1044 Nathues et al. 2019, *The Astronomical Journal* 158, Number 2  
1045  
1046 Nathues et al. (2017), *The Astronomical Journal*, 153:112(12pp).  
1047  
1048 Nathues, A., Schmedemann, N., Thangjam, G. et al. *Nat. Astron.* 4, 794–801 (2020).  
1049 <https://doi.org/10.1038/s41550-020-1146-8>  
1050  
1051 Neesemann, A., Van Gasselt, S., Schmedemann, N., et al. (2019) *Icarus* 320, 60–82.  
1052 <https://doi.org/10.1016/j.icarus.2018.09.006>  
1053  
1054 Neumann, W., et al. (2020) *A&A* 633, id. A117.  
1055  
1056 Neveu M. and Desch S.J., 2015. *Geophysical Research Letters* 42, 10,197-10,206.  
1057  
1058 Neveu, M., Desch, S.J. and Castillo-Rogez, J.C., 2015. *Journal of Geophysical Research: Planets* 120, 123-154.  
1059  
1060 Neveu, M., Desch, S.J. and Castillo-Rogez, J.C. (2017) *Geochimica et Cosmochimica Acta*, 212, 324-371.  
1061  
1062 Nimmo, F., Hamilton, D.P., McKinnon, W.B., et al. (2016) *Nature* 540, 94-96.  
1063  
1064 O'Brien, D.P., Sykes, M.V., 2011. *Space Science Reviews* 163, 41–61. <https://doi.org/10.1007/s11214-011-9808-6>  
1065  
1066 Öberg, K.I. and Wordsworth, R. (2019) *The Astronomical Journal* 158, 194.  
1067 <https://doi.org/10.3847/1538-3881/ab46a8>  
1068  
1069 Onstott, T.C., Lin, L.H., Davidson, M., et al. 2006a. *Geomicrobiology Journal* 23, 369-414.  
1070 <https://doi.org/10.1080/01490450600875688>  
1071  
1072 Onstott, T.C., McGown, D., Kessler, J., et al. (2006b) *Astrobiology* 6, 377-395.  
1073 <https://doi.org/10.1089/ast.2006.6.377>  
1074  
1075 Otto, K.A., et al. (2019) *JGR* 125, 1188-1203.  
1076  
1077 Park, R. S., et al. (2020) *Nature Astronomy* 4, 748-755.  
1078  
1079 [Pikuta, E.V., Hoover, R.B. and Tang, J. \(2007\) \*Critical reviews in microbiology\*, 33, 183-209.](https://doi.org/10.1080/10408410701451948)  
1080  
1081 <https://doi.org/10.1080/10408410701451948>  
1082  
1083 Pizzarello S., et al. (2001) *Science* 293, 2236-39.  
1084  
1085 Pizzarello, S., Holmes, W. (2009) *GCA* 73, 2150–2162. doi:10.1016/j.gca.2009.01.022  
1086  
1087 Pizzarello S. and Williams L. B. 2012. *The Astrophysical Journal* 749:161–167.  
1088  
1089 Platz, T., Nathues, A., Schorghofer, N., et al. (2016) *Nature Astronomy* 1, 1–6.  
1090 <https://doi.org/10.1038/s41550-016-0007>  
1091  
1092 Platz, T., Nathues, A., Sizemore, H.G., Crown, et al. (2018) *Icarus* 316, 140–153.  
1093 <https://doi.org/10.1016/j.icarus.2017.08.001>  
1094  
1095 Postberg et al. 2011 *Nature* 474:620-622.  
1096  
1097 Prettyman T. H., Yamashita N., Toplis M. J., et al. (2017) *Science*, 355, 55-59.  
1098  
1099 Qi, C., et al. (2018) *Geophys. Res. Lett.* 45, 12757-12765. <https://doi.org/10.1029/2018GL080228>  
1100  
1101 Quick, L.C., Glaze, L.S., Baloga, S. M. (2017) *Icarus* 284, 477-488.  
1102  
1103 Quick, L. C., et al. (2019) *Icarus* 320, 119-135.  
1104  
1105 Raponi, A. et al. (2019) *Icarus* 320, 83-96.

- 1096 Raponi, A., De Sanctis, M. C., Frigeri, A., et al. (2018) *Science Advances*, 4(3), 1138-1139. <https://doi.org/10.1126/sciadv.aao3757>
- 1099 Raponi, A., et al. (2017) *Icarus*, 1140-1141. doi:10.1016/j.icarus.2017.10.023.
- 1101 Raponi, A., et al. (2021) *Life* 11, 1142-1143. doi:10.3390/life11010009.
- 1103 Raymond, S.N. and Izidoro, Icarus 297, 134-148 (2017).  
1104 Doi: [10.1016/j.icarus.2017.06.030](https://doi.org/10.1016/j.icarus.2017.06.030).
- 1105 Raymond, S.N., and Nesvorny, D. ArXiv:1146-1147.  
1106 <https://arxiv.org/pdf/2012.07932.pdf>.
- 1107 Raymond, C. A., et al. (2020) *Nature Astron.* 4, 741-747.
- 1108 Reeves, E.P. and Fiebig, J., 2020. *Elements: International Magazine of Mineralogy, Geochemistry, and Petrology* 16, 25-31.  
1109 <https://doi.org/10.2138/gselements.16.1.25>
- 1110 Remusat, L., et al. (2010) *ApJ* 713 1048.
- 1111 Remusat, L. 2015, in *EMU Notes in Mineralogy - Planetary Mineralogy*, ed. M. R. Lee, & H. Leroux (The European Mineralogical Union), 33.
- 1112 Rivkin A. S., Asphaug E., Bottke W. F. (2014) *Icarus* 243, 429-439.
- 1113 Roth, L. (2018) *Icarus* 305, 149-159.
- 1114 Roth, L., Ivchenko, N., Retherford, K. D., et al. (2016) *Geophysical Research Letters*, 43, 2465-2472.  
1115 <https://doi.org/10.1002/2015GL067451>
- 1116 Rousselot, P., Jehin, E., Manfroid, J., et al. (2011) *Astronomical Journal*, 142(4), 1164-1165.  
1117 <https://doi.org/10.1088/0004-6256/142/4/125>
- 1118 Rubin, A. E., Zolensky, M. E., Bodnar, R. J. (2002) *Meteoritics & Planetary Science*, 37, 125-141.
- 1119 Rubin A. E., Trigo-Rodriguez J. M., Huber H., and Wasson J. T. 2007. *Geochimica et Cosmochimica Acta* 71, 2361-2382.
- 1120 Ruesch, O., et al. (2016) *Science* 353, aaf4286.
- 1121 Ruesch, O., et al. (2019a) *Nature Geosci.* 12, 505-509.
- 1122 Ruiz, J., et al., (2019) *Nat. Astron.* 3, 916-921.
- 1123 Ruesch, O., Quick, L.C., Landis, M.E., et al. (2019b) *Icarus* 320, 39-48.
- 1124 Salmon, J., Canup, R. (2018) *Science Adv.* 4, eaar6887.
- 1125 Schenk, P., et al. (2020). *Nature Comm.* 11, 3679.
- 1126 Schenk, P., Castillo-Rogez, J. C., et al. (2021) *Icarus*, <https://doi.org/10.1016/j.icarus.2021.114343>.
- 1127 Schmidt, B. E., Blankenship, D. D., Patterson, W., Schenk, P. (2011) Active chaos formation over shallow subsurface water on Europa, *Nature* 479 502-505.
- 1128 Schmidt, B.E., Hughson, K.H.G., Chilton, H.T., et al. (2017) *Nature Geosci* 10, 338-343. <https://doi.org/10.1038/ngeo2936>
- 1129 Schmidt, B., et al. (2020) Post-impact cryo-hydrologic formation of small mounds and hills in Ceres' Occator Crater, *Nature Geosci.* 13, 605-610.
- 1130 Schmitt-Kopplin et al, 2010, which indeed show the presence of thousand compounds in the SOM. <https://www.pnas.org/content/107/7/2763.short>
- 1131 Schörghofer, N., Mazarico, E., Platz, et al., (2016). *Geophysical Research Letters*, 43, 6783-6789. <https://doi.org/10.1002/2016GL069368>
- 1132 Scully, J. E. C., et al. (2018) *Icarus* 316, 46-62.
- 1133 Scully, J.E.C., Buczkowski, D.L., Schmedemann, N., et al., 2017. *Geophysical Research Letters* 44, 9564-9572. <https://doi.org/10.1002/2017GL075086>
- 1134 Scully, J. E. C., et al. (2020) *Nature Comm.* 11, 3680.
- 1135 Scully, J., et al., submitted to the *Planetary Science Journal*.
- 1136 Seewald, J.S., Benitez-Nelson, B.C. and Whelan, J.K., 1998. *Geochimica et Cosmochimica Acta* 62, 1599-1617. [https://doi.org/10.1016/S0016-7037\(98\)00000-3](https://doi.org/10.1016/S0016-7037(98)00000-3)
- 1137 Shi, X., et al. (2019) GAUSS -- A Sample Return Mission to Ceres, *White Paper to ESA's Voyage 2050*.
- 1138 Sherwood Lollar, B.S., Westgate, T.D., Ward, J.A., Slater, G.F. and Lacrampe-Couloume, G., 2002. *Nature* 416, 522-524. <https://doi.org/10.1038/416522a>
- 1139 Sherwood Lollar, B., Heuer, V. B., McDermott, J., et al., 2021. *Geochimica et Cosmochimica Acta* 294, 295-314. <https://doi.org/10.1016/j.gca.2020.11.026>
- 1140 Shock, E.L. and McKinnon, W.B. (1993) *Icarus* 106, 464-477. <https://doi.org/10.1006/icar.1993.1185>
- 1141 Sirono, S. (2013) *Earth Planets Space*, 65, 1563-1568.
- 1142 Siskin, M., Katritzky, A. R., 2001. *Reactivity of Chemical Reviews* 101, 825-835. <https://doi.org/10.1021/cr000088z>
- 1143 Schenk, P. M., et al (2019). *Icarus* 320, 159-187

- 1179 Sizemore H. G., Schmidt B. E., Buczkowski D. A., et al.  
1180 (2019) *J. Geophys. Res. - Planets* 124, 1650-1689.  
1181 <https://doi.org/10.1029/2018JE005699>
- 1182 Sori, M., et al. (2017), *Geophys. Res. Lett.* 44, 1243–  
1183 1250.
- 1184 Sori, M., et al. (2018) *Nature Astron.* 2:946-950.
- 1185 Spencer, J., Nimmo, F. (2013) *AREPS* 41, 693-717.
- 1186 Stephan, K., et al. (2018) *MAPS* 53, 1866-1883.
- 1187 Thangjam et al. 2016, *The Astrophysical Journal Letters*,  
1188 833:L25(9pp), doi:10.3847/2041-8213/833/2/L25
- 1189 Thomas, E.C., Vu, T.H., Hodyss, R., Johnson, P.V. and  
1190 Choukroun, M. (2019) *Icarus* 320, 150-158.  
1191 <https://doi.org/10.1016/j.icarus.2017.12.038>
- 1192 Travis, B.J., Bland, P.A., Feldman, W.C. and Sykes,  
1193 M.V., 2018. *Meteoritics & Planetary Science* 53, 2008-  
1194 2032. <https://doi.org/10.1111/maps.13138>
- 1195 Vernazza, P., et al. (2017) *Astron. J.* 153, 72.
- 1196 Villarreal, M. N., Russell, C. T., Luhmann, J. G., et al.  
1197 (2017) *The Astrophysical Journal Letters*, 838(1).  
1198 <https://doi.org/10.3847/2041-8213/aa66cd/>
- 1199 Vinogradoff, V., et al. (2017) *Geochimica et*  
1200 *Cosmochimica Acta* 212, 234-252.
- 1201 Vinogradoff, V. et al. (2018) *Icarus* 305, 358-370.
- 1202 Vinogradoff et al., 2020, *Geochimica et Cosmochimica*  
1203 *Acta* 269 150-166.
- 1204 Waite, J.H., Glein, C.R., Perryman, R.S., et al. (2017)  
1205 *Science* 356, 155-159.  
1206 <https://doi.org/10.1126/science.aai8703>
- 1207 Williams, D., et al. (2018) *Icarus* 316, 1-13.
- 1208 Zambon, F., et al. (2017) *Geophys. Res. Lett.* 44, 97-104.  
1209 <https://doi.org/10.1002/2016GL071303>
- 1210 Zolotov, M. Y. (2020) *Icarus* 135, 113404.
- 1211